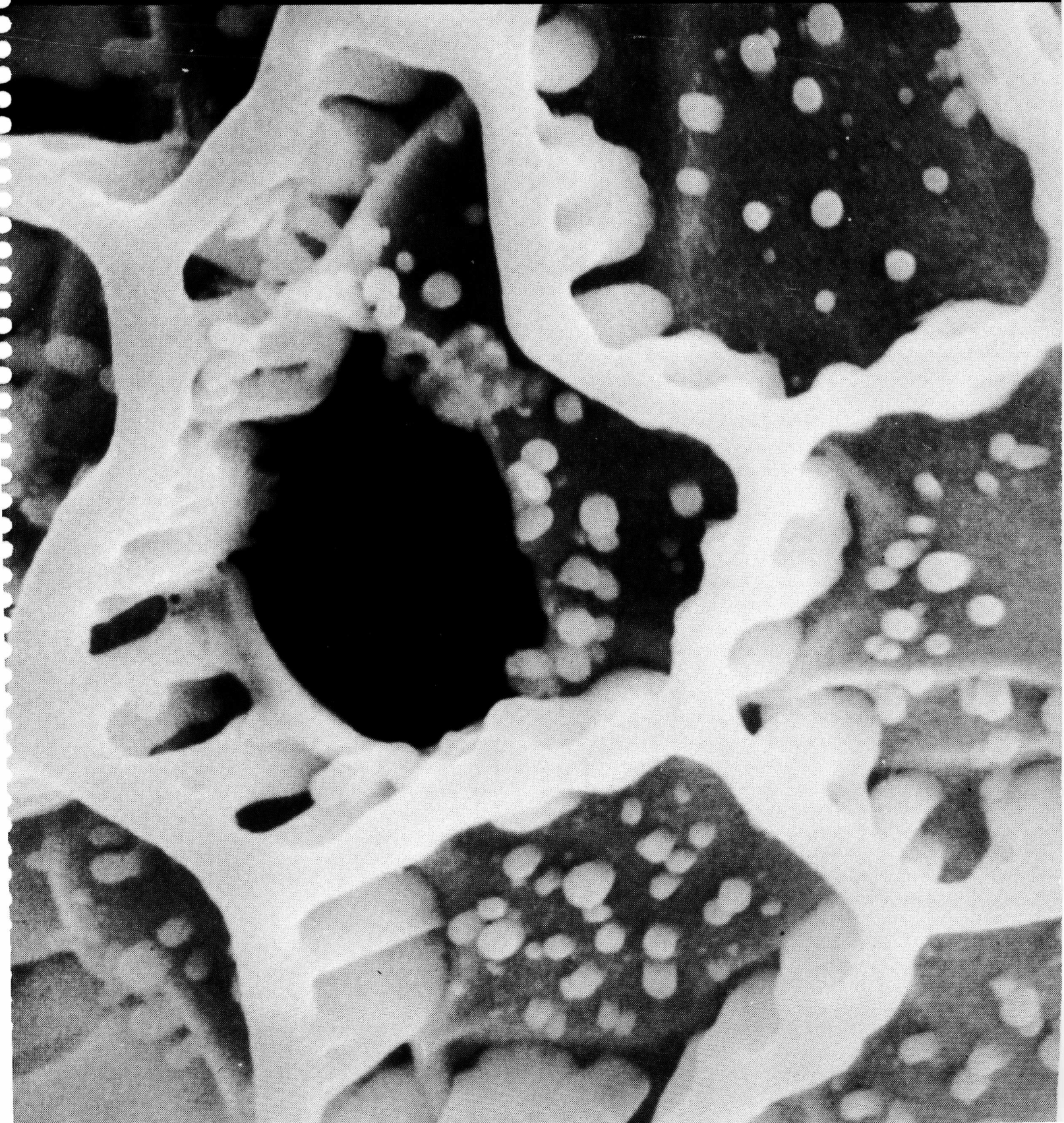


RHODES COLLEGE
FOUNDED 1848

Science Journal

Volume X

May 1992



THE RHODES COLLEGE SCIENCE JOURNAL

VOLUME X

May 1992

PREFACE

The Rhodes College Science Journal is a student-edited, annual publication which recognizes the scientific achievements of Rhodes students. Founded nine years ago as a scholarly forum for student research and scientific ideas, the journal aims to maintain and stimulate the tradition of independent study. We hope that in reading the journal, other students will be encouraged to pursue scientific investigations and research.

Editor

Anne Finney

Asst. Editor

Kristen Lichtermann

Staff

Anna Becher

Nancy Turner

Trey White

Acknowledgements

Dr. David Kesler

The Rhodes Science Initiative

Alumni and friends whose generosity
has made this publication possible

Cover photo: SEM of the surface of a pollen
grain of *Ruellia ciliosa* by Julie Olsen

Contents

Anna M. Becher

Inheritance Studies of Esterase Enzymes in the German
Cockroach, *Blattella Germanica*

Dr. B. Jones, advisor

J. B. Diestelhorst and B. W. Walker

Magnolia Leaf and Root Extracts Inhibit Seed Germination

Dr. C. Stinemetz, advisor

Valerie S. Scott

The Effects of Masticatory Forces on Sutural Development in Rats,
Rattus Norvegicus

Dr. C. Jaslow, advisor

Kathy L. Wheeler

The Biological Activity of Two Chloramphenicol Derivatives

Dr. H. Parish, advisor

Trey White

Solar Ca K Irradiance Variations Through One Solar Rotation

Dr. J. Streete, advisor

INHERITANCE STUDIES OF ESTERASE ENZYMES IN THE GERMAN COCKROACH, *BLATTELLA GERMANICA*

ANNA M. BECHER

ABSTRACT

Polyacrylamide gel electrophoresis (PAGE) was used to study the inheritance pattern of esterase allozymes in a laboratory strain of the German cockroach. The purpose of this study was to determine the allelic inheritance of a set of allozymes in the Pike strain. Many single matings between male and virgin female Pike cockroaches were set up. The nymphs from each of these matings were homogenized in Peacock buffer after their third or fourth instar stage (weight 60mg). The male and female parents were homogenized at the same time as their nymphs. Extracts from the homogenized cockroaches were then electrophoresed. Preliminary studies show that there are three forms of expression: a single fast band, a single slow band, and a heterozygous doublet. We have hypothesized that there are three alleles at a single locus determining the set of allozymes' inheritance pattern.

INTRODUCTION

Polyacrylamide gel electrophoresis (PAGE) is used to separate many biological molecules. In German cockroach studies, PAGE has been used to separate the roach's esterases. PAGE uses a constant electrical current to move the esterases from a negative pole to a positive pole in a vertical slab unit. The esterases move according to their charge and weight; the esterases (represented as dark bands after the staining procedure) at the bottom of the gel are faster moving than the esterase bands at the top of the gel.

The purpose of this study is to determine the allelic inheritance of an allozyme in a particular strain of *Blattella germanica*. With observation of PAGE gels of the Pike strain, a doublet of esterase bands was noticed (Figure). According to Narang's work, this doublet is a set of allozymes. Using electrophoretic work done on the house fly (*Musca domestica* L), Narang determined that doublets were allozymes; an allozyme being an esterase that has several forms of expression (Narang, 1976). With the Pike strain there are three forms of expression: fast single, slow single, and heterozygous (a doublet of a fast and a slow band). Using single pair matings, PAGE was used to determine the inheritance pattern of the allozyme.

MATERIALS AND METHODS

The Pike strain of *B. germanica* was collected by Jennifer Burrow in the spring of 1989 from the Pi Kappa Alpha fraternity house at Rhodes College in Memphis, TN. The Pike strain has been housed in a lard-like container (two feet by one foot) in an incubator kept at 68 degrees C. Cage grease (a mixture of Vaseline and mineral oil) was used to keep the roaches from climbing up the sides of the bucket. Virgin females and males were collected from a smaller culture that was taken from the big culture. Three to five virgin females were put in a small container with one virgin male. The container was covered with wire gauze; two pellets of dog food and a small beaker of water in a small petri dish were placed in the container. Later small pieces of cardboard were added for

the nymphs to live in. After three weeks, the pregnant females were placed in individual containers. After the females dropped their egg cases and the nymphs aged for at least three weeks, the female parent, most of the nymphs, and male parent were killed.

All roaches were homogenized using a screw driver homogenizer and Peacock buffer. Each roach was weighed first and then homogenized in 4 ul of Peacock buffer per mg of weight in a microcentrifuge tube. The homogenate was then centrifuged for ten minutes. Cook and Forgash showed that homogenized roaches could be refrigerated after this step for at least seventy-two hours and still show esterase activity, but we observed activity after one week of refrigeration (Cook, 1965). After centrifuging, tracking dye was added to a portion of the homogenate. The mixture of tracking dye to homogenate was 2:3.

A 7.5 % polyacrylamide running gel was prepared in the Hoeffer SI 600 Se vertical slab unit. A 5 % focusing gel was prepared and a 1.5 mm comb was inserted. The homogenate-tracking dye solution was loaded into the wells of the gel. Samples of 15 ul were loaded into a fifteen well gels, and samples of 10 ul were loaded into a twenty well gels. A standard of carboxylic-ester hydrolase from Porcine liver (from Sigma Chemical company, stock number E-3128) was used for Rm values to be determined. 10 ul of the standard was diluted in 10 mL of Peacock buffer. The standard was mixed in a 2:1 ratio with tracking dye.

The gels were then transferred to the upper chamber unit and placed in the buffer chamber. Peacock buffer was added to the upper chamber, water was run through the cooling chamber, and the electrical leads were hooked up to the chamber. The electrical current was set at sixty volts for two gels and thirty volts for one gel and allowed to run for two hours and thirty minutes with voltage varying.

After disassembly of the gel apparatus, gels were soaked in an alpha acetate and RR Fast Blue dye for fifteen minutes at maximum. Gels were then stored in 7% acetic acid.

RESULTS

Data from three major crosses have been collected. The parents of cross 1 both had the single slow band phenotype for this allozyme set. All of the first generation tested, 17 roaches, also had the single slow band phenotype. In cross 2, the male parent had the single slow band phenotype while the female parent had the heterozygous doublet phenotype (a combination of slow and fast bands). 6 of the first generation had the single fast band, 23 roaches had the single fast band, and 9 of the first generation roaches had the doublet heterozygous band. There were 38 roaches in the first generation of cross 2. In cross 3, both the female and male parents were single slow phenotype. All of the first generation, 28 roaches, were of the single slow phenotype.

CONCLUSIONS

Although the data is low in numbers, I have attempted to determine the mode of inheritance of this allozyme. In cross 2 there are six fast band progeny. This brings a serious problem; how does a fast single band arise from a single slow male and a heterozygous female? Assuming the male parent is $E^S E^S$ (E = esterase) and the female is

ESES, it is not possible to produce EFES (heterozygous), as Punnett square shows:

male		ES	ES
female	EF	EFES	EFES
	ES	ESES	ESES

Therefore, the male parent must have a null allele, EO, instead of having ESES. If the male parent had a null allele, the Punnett square would look like:

male		ES	EO
female	EF	EFES	EFEO
	ES	ESES	ESEO

This pattern would give rise to fifty percent of the progeny being slow single band (ESES or ESEO), twenty-five percent being fast single band (EFEO), and twenty-five percent of the progeny being heterozygous (EFES). A chi square test will prove this theory acceptable.

	observed #	expected #	χ^2
fast single band	6	9.5	1.3
slow single band	23	19	0.80
heterozygous band	9	9.5	0.03
total	38	38	2.13

(see Table for data)

χ^2 with two degrees of freedom is 5.99

Therefore, the hypothesis of the male parent having a genotype of ESEO is accepted since 2.13 is less than 5.99. Because of this hypothesis, there should be some slow bands in the progeny that are lighter in intensity than other slow bands, due to the null allele. These light slow bands should have the same intensity as the fast single band. With the staining procedure used here, it is hard to compare two different gels to see if there are differences in the band intensities, but there appears to be a difference in bands of the same gel.

In crosses 2 and 3, all of the progeny have slow single bands. The female parent has a slow single band phenotype in both crosses. The female parent could have either ESEO or ESES genotype. The male parent for crosses #2 and #3 is the same male from cross #1 (ESEO). A Punnett square for cross #2, assuming the female parent is ESEO is:

male		ES	EO
female	ES	ESES	ESEO
	EO	ESEO	EOEO

If the female parent is ESEO, then twenty-five percent of the progeny would not have any band pattern for this allozyme. Narang et al have found that a house fly with a esterase genotype ESEO crossed with another ESEO house fly gave a progeny of about seventy-five percent slow and twenty-five percent null (Narang, 1976). In all of the PAGE gels, there were no blanks for this allozyme; this signifies that the female parent is

ESES. A Punnett square shows:

male		ES	EO
female	ES	ESES	ESEO
	ES	ESES	ESEO

In this case, all of the progeny are slow, which is observed (see table #2). The same hypothesis is true for cross 3. Because the male parent is, the female parent must be ESES. If the female parent is not ESES, but ESEO, then there would be blank bands for this allozyme in the cross 3 progeny. This phenomena is not observed; all progeny have slow single bands.

With this data, it is hypothesized that there are three alleles that determine the studied allozyme's inheritance pattern. These three alleles are fast, slow, and null. Combinations of these alleles can be slow (ESEO or ESES), fast (EFEO or EFEF), and heterozygous (EFES). Narang et al have proven this hypothesis to be true with their PAGE work on house fly esterases (Narang, 1976).

REFERENCES

- Cook, B. J. and A. J. Forgash. (1965). "The identification and distribution of the carboxylic esterases in the American cockroach, *Periplaneta americana* (L.)" *Journal of Insect Physiology* 11: 237 -250.
- Narang, S., A.C. Terranova, I.C. McDonald, and R.A. Leopold. (1976). "Esterases of the house fly." *Journal of Heredity* 67: 30 - 38.

Table 1. Cross 1 - Pike male * Pike female (as recorded from the PAGE gel)

	single fast band	single slow band	heterozygous (double)
male parent	0	*	0
female parent	0	*	0
nymphs	0	17	0

Table 2. Cross 2 - Pike male * Pike female

	single fast band	single slow band	heterozygous (double)
male parent	0	*	0
female parent	0	0	*
nymphs	6	23	9

Table 3. Cross 3 - Pike male * Pike female

	single fast band	single slow band	heterozygous (double)
male parent	0	*	0
female parent	0	*	0
nymphs	0	28	0

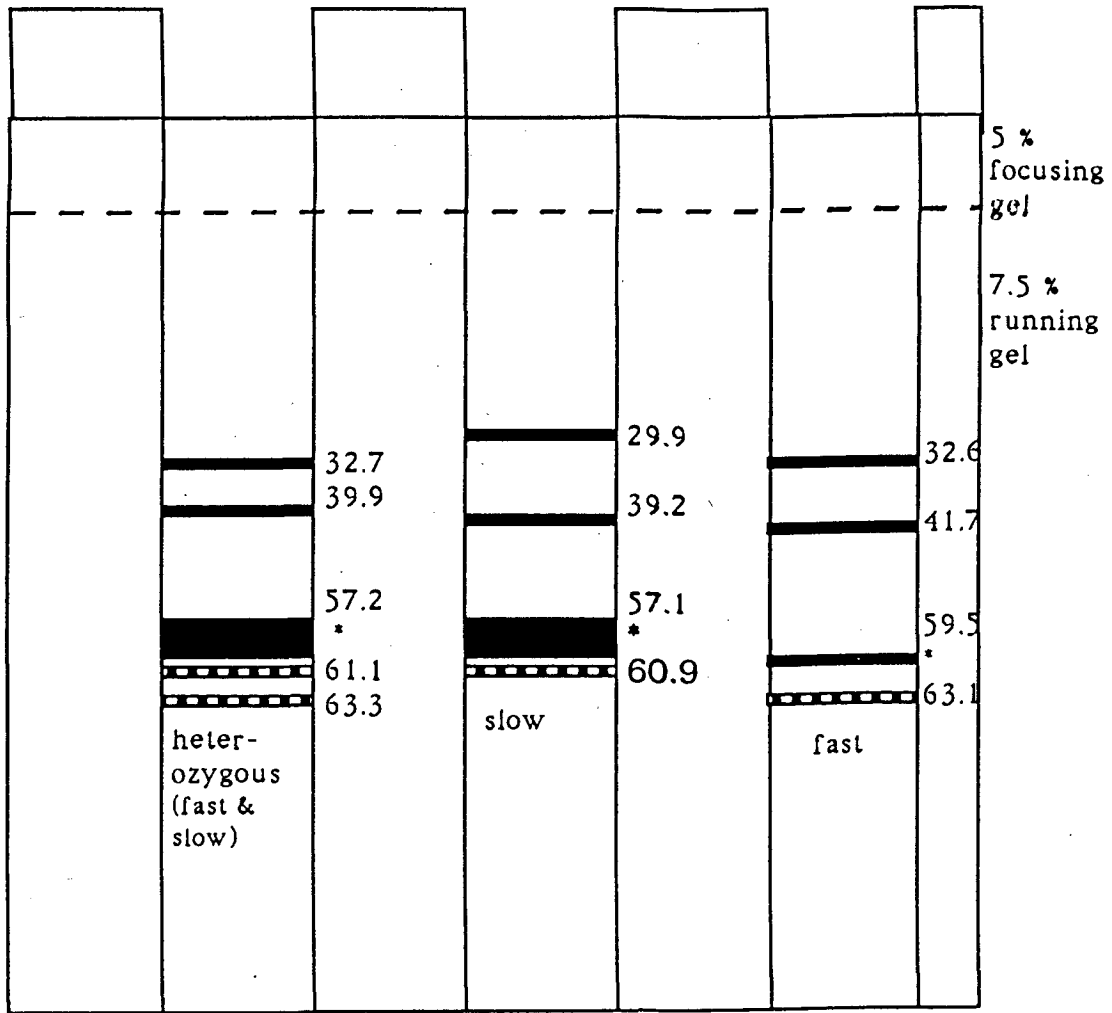


Figure. The studied allozyme pattern (dotted pattern bands) of Pike roaches as seen in PAGE gel [measured in mm with porcine liver esterase as standard]. * is a smear.

MAGNOLIA LEAF AND ROOT EXTRACTS INHIBIT SEED GERMINATION

J.B. DIESTELHORST AND B.W. WALKER

ABSTRACT

The base of southern magnolia trees (Magnolia grandiflora L.) are devoid of most grasses. This absence of grasses may be due to a lack of light, moisture, or some chemical released from the magnolia. We have investigated the possibility that southern magnolia trees release a chemical which delays or inhibits the germination of rye, bluegrass and barley. We found that germination of all types of grass seeds were inhibited by magnolia root and leaf extracts. Boiling samples did not alter the inhibitory effect of the extracts on seed germination. Also, seeds planted in soil on a transect from the base of the tree to the dripline of the tree exhibit lower germination rates near the base than seeds planted in soils originating outside the dripline. Preliminary studies have suggested that one possible means through which the extract interferes with seed germination is by inhibiting the activity of alpha amylase in germinating seeds. These studies suggest that Magnolia grandiflora L. releases an alleopathic substance into the soil which inhibits the germination of grass seeds.

INTRODUCTION

We have noticed that most lawn grasses are not present around the Southern Magnolia (*Magnolia grandiflora* L.) tree. However, tufts of rye grass as well as some dicot weeds do appear underneath these trees. The lack of most lawn grasses could be due to an inhibition of seed germination, unfavorable environmental conditions which might interfere with the establishment and continued existence of seedlings, or both of the above. We have chosen to investigate the first possibility, that seed germination of most lawn grasses is inhibited. Three possible explanations for why most lawn grasses do not appear underneath Southern Magnolia trees occurred to us: lack of light necessary for activation of phytochrome due to a heavy year around leaf canopy, lack of moisture due to the shedding of water to the periphery of the tree, the release or leeching of an alleopathic substance (Rice, 1979) from the tree which interferes with some aspect of seed germination. In this study, we have investigated the latter possibility by: 1) determining if leaves and roots of magnolia contain a substance which selectively inhibits the germination of Kentucky-31 bluegrass (KY-31) relative to rye grass, 2) examining the germination rate of KY-31 and rye grass in soils sampled from the base of a magnolia tree and radiating outwards, and 3) determining if the action of a magnolia seed germination inhibitor acts through interfering with alpha-amylase action, synthesis, or release from the aleurone layer (Ashford, 1984).

MATERIALS AND METHODS

Plant and Soil Materials Leaves were collected from a Magnolia tree (approximately 30 years old) on the Rhodes College campus which was devoid of most lawn grasses underneath the canopy but surrounded by a mixture of lawn grasses, principally K-31. Soil samples were also collected from around this tree. Roots tissue was

collected from a 5-year old tree purchased from a local nursery. KY-31 and annual rye grass seed was also purchased locally. Barley seeds were purchased from Carolina Biological.

Preparation of Leaf and Root Extracts Deveined leaves and roots were weighed and homogenized in 100 ml of distilled water and then vacuum filtered with #1 Whatman filter paper. The pH of the extracts was determined and a distilled water solution was adjusted with HCl and NaOH. All the extracts were adjusted to the pH of the 80 g/100 ml extracts. Extracts were stored in the refrigerator and discarded after 1 week.

Seed Germination Assays in Extract Solutions Seeds were surface sterilized in 15% Clorox and rinsed with distilled water. Twenty seeds were placed in petri dishes containing a disc of #1 Whatman filter paper and 15 ml of extract solution or pH adjusted distilled water. Heated samples were boiled for 5 minutes. After 5 days the % germination of seeds was determined.

Seed Germination Assays in Soil Samples Soil samples were collected beginning at the base of the tree and extending outwards in increments of 1.5 meters up to 7.5 meters from the base. KY-31 and rye grass seeds were marked with two different fluorescent paints and sown in petri dishes containing 50 g of wetted soil. Germination of seeds was determined after 10 days.

Determination of Alpha-Amylase Enzyme Activity in Aleurone Layers Treated with Magnolia Extracts Half seeds (lacking the embryo) were surface sterilized and incubated on wetted vermiculite. After 1 week the aleurone layers were removed and placed in an incubation buffer with or without extract (Table 1). The aleurone layers were allowed to incubate for 24 hours and then 100 ul samples were withdrawn and stored at -80 C. The activity (1) and protein content (2) of these samples were determined.

RESULTS

Leaf extracts inhibit seed germination in a concentration-dependent fashion (Figure 1) and the germination of rye, barley, and K-31 seeds were all affected by the leaf extracts with K-31 being considerably more sensitive to leaf extract than rye grass. Heating the extract slightly enhanced the inhibitory effect of the extract (Figure 2).

Results similar to those found with leaf extracts were found when seeds were treated with root extracts (Figure 3). However, root extracts were not as effective as the leaf extracts at inhibiting germination of seeds. Boiling root extracts also slightly increased the inhibitory effect of the extracts (Figure 4).

A relationship between the distance from the base of the tree and the per cent germination was found (Figure 5). Seeds placed in soils collected near the base of the tree had a lower % germination after 10 days than seeds placed in soils collected from the periphery of the transect. The germination of KY-31 was more sensitive than rye grass to the inhibitory effect of the soils on seed germination.

Both magnolia leaf and root extracts interfered with the activity of alpha-amylase released from the aleurone layer of seeds (Table). The extracts inhibited the activity of alpha-amylase and did not alter either the synthesis or release of the enzyme (data not shown). A correlation can be noted between the effectiveness of extracts to inhibit alpha-amylase activity and the effect of the extracts on seed germination.

CONCLUSIONS

Extracts from leaves and roots of Southern Magnolia inhibit the germination of lawn grasses, and soils closest to the base of the tree have lower seed germination.

The inhibitory substance in the extract is not affected by heat thus it is unlikely that it is a protein.

Root and leaf extracts interfere with alpha-amylase activity.

One possible explanation for the lack of most lawn grasses around magnolia may be that the tree releases an alleopathic compound which inhibits the germination of grass seeds; this alleopathic substance may alter seed germination by inhibiting the activity of alpha-amylase.

REFERENCES

- Ashford, A.E. and F. Gubler. (1984). "Mobilization of polysaccharide reserves from endosperm." IN : Seed Physiology Vol. 2, D Murray, ed. Academic Press, NY.
Bradford, MN. (1976) "A rapid and sensitive method for the quantitation of microgram quantities of protein utilizing the principle of protein dye binding." *Anal. Biochem.* 72:248-254.
Rice, EL. (1979). "Alleopathy-- An update." *The Botanical Review* 45:15-109.

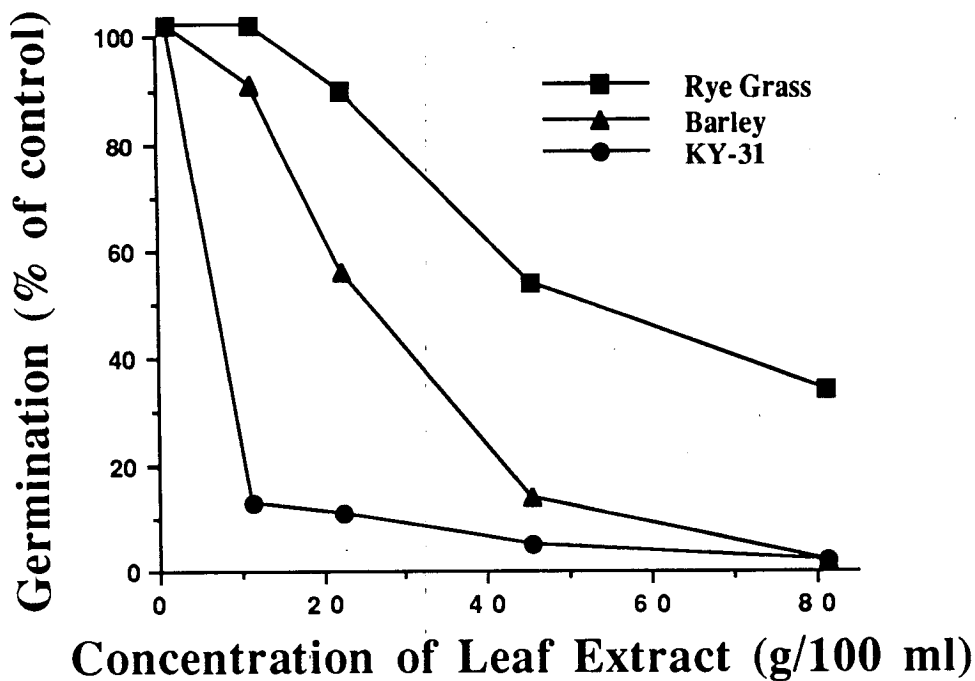


Figure 1. THE EFFECT OF SOUTHERN MAGNOLIA LEAF EXTRACTS ON SEED GERMINATION. Seeds were sown on petri dishes containing differing concentrations of leaf extracts. The pH of extracts was adjusted to 5.9 with HCl and NaOH.

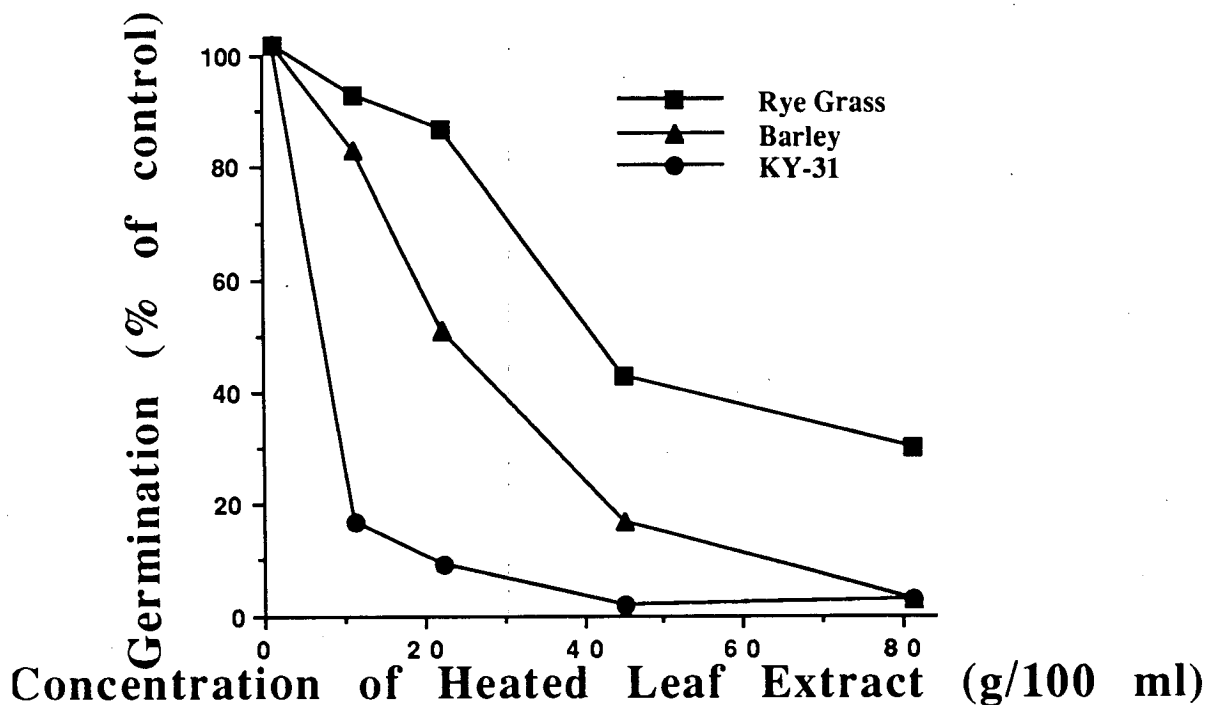


Figure 2. THE EFFECT OF SOUTHERN MAGNOLIA LEAF EXTRACTS ON SEED GERMINATION AFTER HEATING. Seeds were sown on petri dishes containing differing concentrations of leaf extracts which had been boiled for 5 minutes and then allowed to cool. The pH of extracts was adjusted to 5.9 with HCl and NaOH.

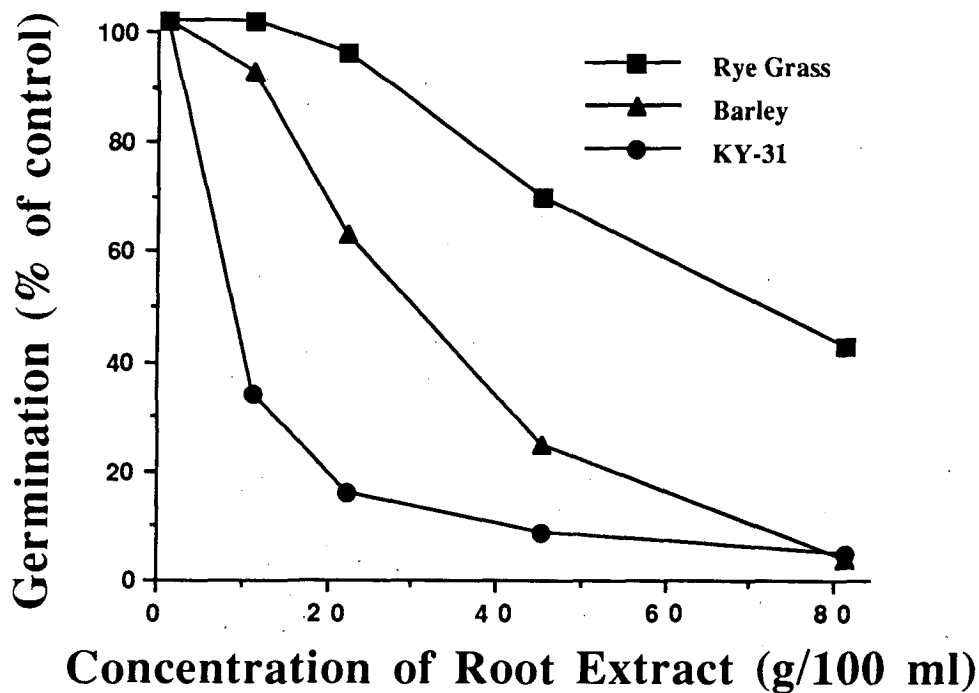


Figure 3. THE EFFECT OF SOUTHERN MAGNOLIA ROOT EXTRACTS ON SEED GERMINATION. Seeds were sown on petri dishes containing differing concentrations of root extracts. The pH of extracts was adjusted to 6.2 with HCl and NaOH.

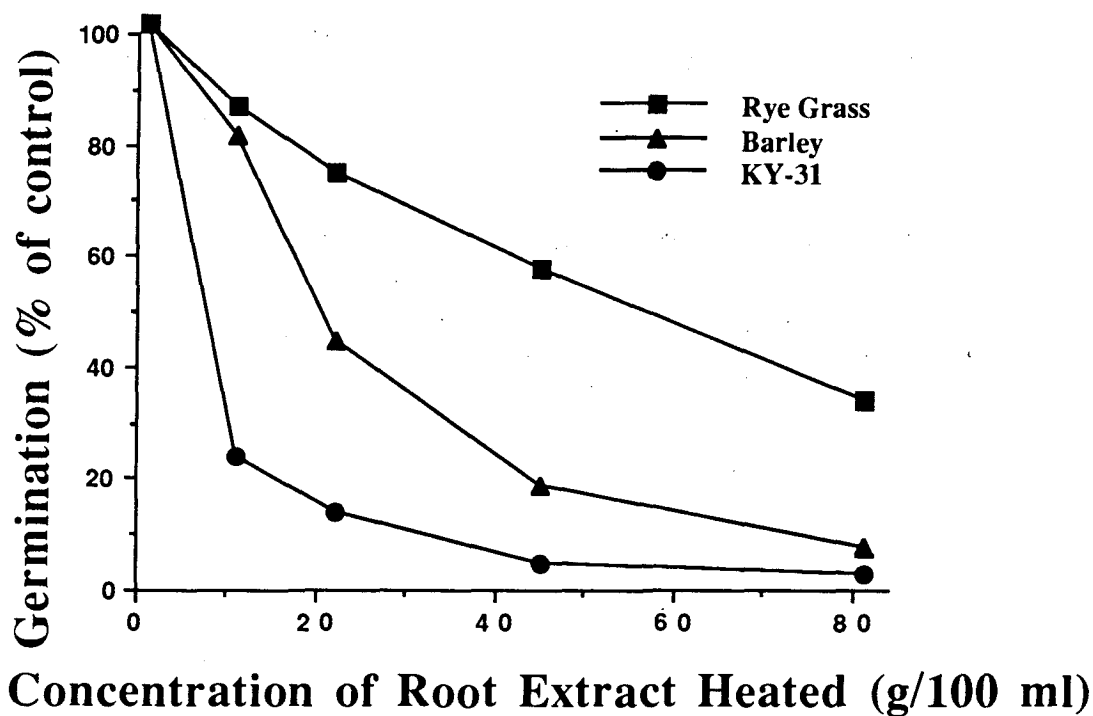


Figure 4. THE EFFECT OF SOUTHERN MAGNOLIA LEAF EXTRACTS ON SEED GERMINATION AFTER HEATING. Seeds were sown on petri dishes containing differing concentrations of root extracts which had been boiled for 5 minutes and then allowed to cool. The pH of extracts was adjusted to 6.2 with HCl and NaOH.

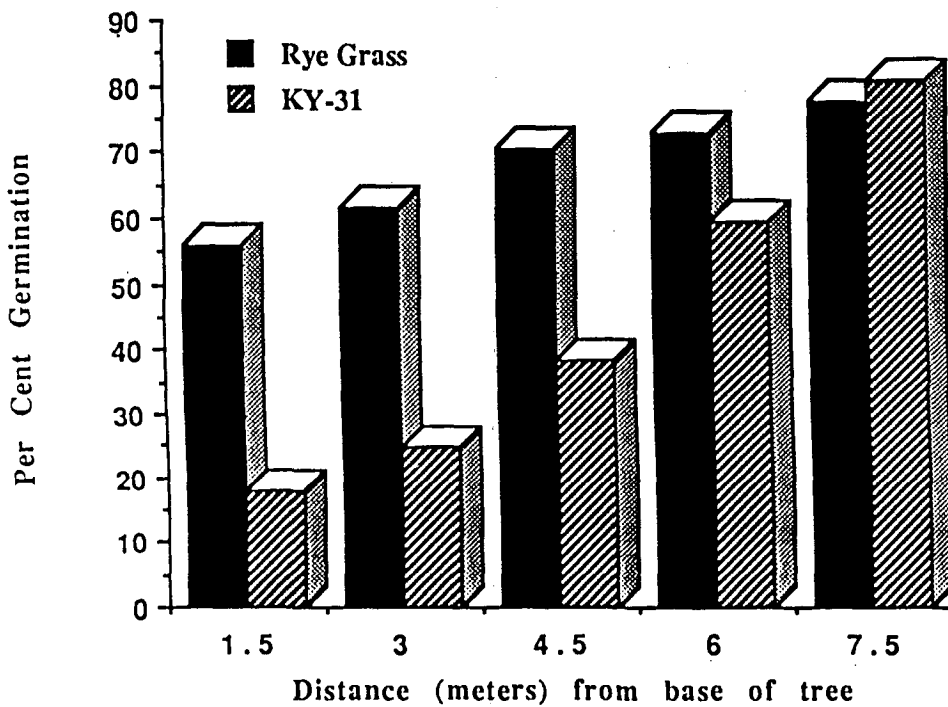


Figure 5. THE GERMINATION OF SEEDS IN SOILS AROUND A SOUTHERN MAGNOLIA. A transect was constructed beginning at the base of a magnolia tree and extending outwards to 7.5 meters. Soils were collected at 1.5 meter increments and seeds sown in these soils. After 10 days the per cent germination was determined.

Table. THE EFFECT OF MAGNOLIA ROOT AND LEAF EXTRACTS ON ALPHA-AMYLASE ACTIVITY. Ten aleurone layers of half seeds were removed and placed in MES buffer solutions, some of which contained root and leaf extracts from magnolia leaves. After 24 hours, samples were removed from the incubation solutions and the activity of alpha-amylase as well as protein content was determined.

Incubation Solution	Units/ml	Units/ml/mg protein
BARLEY:		
Buffer Only	29.70	144.50
Buffer + Leaf Extract *	2.25	3.97
Buffer + Root Extract	2.84	5.72
RYEGRASS:		
Buffer Only	8.13	113.61
Buffer + Leaf Extract	3.46	26.40
Buffer + Root Extract	3.62	32.86
KY-31:		
Buffer Only	8.49	104.77
Buffer + Leaf Extract	0.35	4.45
Buffer + Root Extract	0.54	8.96

* Extract concentration tested equaled 80.42 g/100 ml

THE EFFECTS OF MASTICATORY FORCES ON SUTURAL DEVELOPMENT IN RATS, *Rattus Norvegicus*

VALERIE S. SCOTT

ABSTRACT

*Increased interdigitation of cranial sutures provides a mechanical advantage to the skull, but it is not known whether these increases are genetically programmed or developmentally induced. To address this question, we quantified the degree of sutural interdigitation (complexity) occurring in rats (*Rattus norvegicus*) after exposure to different levels of imposed bite forces during development. Six groups of two rats each were fed diets ranging from a liquid diet to a hard diet of standard rat chow with supplementary hard objects to chew. Eleven sutures in each of the rat skulls were traced and digitized on the computer using a ratio of length over distance to determine complexity. In addition, sutural complexity from 38 wild rat skulls was measured for comparison and to determine natural variation. Five of the 11 sutures in the experimental rats were significantly different than those in the wild rats, but complexity did not increase according to diet among the different sutures. These results indicate that the sutures in the experimental rats were not developmentally induced to show patterns of increased interdigitation that ranged from the liquid to the hard diet.*

INTRODUCTION

The role of complexity of the cranial sutures and the forces that produce interdigitation patterns have fascinated biologists for many years (Jaslow, 1989). Cranial sutures are joints of connective tissue that join the neighboring bones in the skulls of mammals and other vertebrates. The periosteum is the lining on the bones responsible for the connection and the binding of the bones to one another. Previous studies have shown that cranial sutures in mammals have a variable morphology (Massler & Schour, 1951; Moss, 1957, 1961; Moss & Young, 1960). This morphology shows many levels of complexity, ranging from simple straightline sutures to very complex highly interdigitated sutures. Many argue that the complexity of sutures is directly related to the animal's behavior; therefore, form would be directly related to function. While it is not clear how these interdigitations develop, experimental evidence indicates that some portion of sutural morphology is directly influenced by extrinsic forces (Moss, 1957). For example, the forces produced during biting may be responsible for modifying the development and complexity of some of the cranial sutures in the anterior portion of the skull. We hypothesize that the pressure applied to the suture from the use of the incisors will directly effect the complexity of the sutures.

While increased interdigitation is known to provide a mechanical advantage to the skull, it is not known whether these interdigitations are "genetically programmed" or developmentally induced (Jaslow, 1989; Jaslow, 1990; Moss, 1957). If this question can be resolved, this information will be helpful in the understanding of cranial functional morphology, particularly in fossil specimens where there is no record of the types of forces applied to the skull.

We assume that a rodent eating rat chow is applying forces to its skull that are similar to those that would occur in the wild. During gnawing, the forces would be

directed from the incisors to the frontonasal, frontopremaxillary and frontomaxillary sutures. In order to attempt to manipulate the complexity of anterior and posterior sutures in the skull, the rats were fed different consistencies of food. It is assumed that the forces transmitted from the teeth through the skull will increase with the increases in the hard consistency of the diet.

In order to fully investigate the question of whether or not the sutures are "genetically programmed" or developmentally induced, (Jaslow, 1989; Oudhof, 1982) one must do extensive comparative as well as experimental research. We decided to compare sutures from the groups of experimental rats not only to one another, but to also to sutures from a population of wild rats. If in fact there are differences among the groups, these differences can be used to determine if sutural complexity has been genetically programmed or developmentally induced. By comparing the six different groups of experimental rats, one will be able to recognize the significance of various diets and their effects on the complexity of the sutures.

The primary goal of this preliminary study is to attempt to quantify the degree of sutural complexity caused by different levels of imposed forces during development. The secondary goal involves analyzing the sutures from a population of wild rats and comparing the complexity of their sutures to the experimental group of rats that have been developmentally controlled.

MATERIALS AND METHODS

Rattus norvegicus, a standard white lab rat, was used for this pilot study because this rat has a brief period of development, and they have sutures that are most likely to be affected by masticatory forces. The sutures of the rats were also easily measured and digitized on the computer.

In this pilot study only a small number of rats were used. Groups of two rats each were fed diets ranging from a liquid diet to a hard diet of standard rat chow with supplementary hard objects to chew (Table). The first group was fed a liquid diet of vanilla flavored Ensure every day. When the rats were young they ate approximately 60 milliliters a day. As the rats developed, the amount steadily increased and the adult rats were eating 100 milliliters a day by the end of a four month period of time. The Ensure did not have sufficient minerals for the developing rats, therefore the rats on the liquid diet had 0.4 grams of mineral supplement added to 100 milligrams of water every other day or as needed. This group of rats also had their incisors clipped every two weeks for the last month of the experiment. The clipping of the incisors prevented the rats from harming themselves by their lengthy incisors, and it also prevented the rats from grinding their teeth in the absence of food which would have created unwanted bite forces. The second group of rats were also fed a liquid diet of vanilla flavored Ensure. These rats were fed the same amounts and were also given the mineral supplement in the water as needed. The third group ate a soft diet which consisted of powdered standard rat chow mixed with water. Early in their development the rats were fed 10 grams of powdered food mixed with 3 milliliters of water. Again the amount was steadily increased as the rats grew. In their adult stage the rats consumed 30 grams of food mixed with 9 milliliters of water. The rats on the soft food diet were given water as needed. The first three groups had the lids of their cages wired with copper wire to prevent the rats from applying any force to their incisors by gnawing on the bars of the cages. The fourth group of rats ate soft food with hard particles. As juveniles, these rats ate 10 grams the powdered standard rat chow mixed with 3 milliliters of water along with 5 grams of

"grapenuts" cereal mixed into the soft food. When the fourth group reached full development they were eating 25 grams of soft food mixed with approximately 10 milliliters of water along with 7 grams of grapenuts. The amount of grapenuts were not steadily increased, because the rats seemed to devour the cereal. It came to a point where they were ignoring the soft food and only consuming the grapenuts. Grapenuts were selected because of their unique size. It was assumed that the rats would use their molars rather than their incisors to chew the grapenuts. Group five ate a hard diet of the standard rat chow. The sixth group ate a hard diet of rat chow with supplementary wood blocks placed inside the cage that they could chew on at any time. Groups four, five, and six were given water as needed.

During the development of the experimental rats, we conducted extensive comparative research. The comparative research was done with 38 wild rat skulls. There were 25 males and 13 females. Having done a t-test on the sutures and a Mann-Whitney test on one of the sutures, it was obvious that there was no difference between the males and the females. Because there was no significant difference, the male skulls were used to compare the sutures to those of the experimental male rats. The wild rat skulls were on loan from The Memphis State University Museum. These rats were trapped in different areas in Memphis as well as some areas of Mississippi. The results of this comparative research served as a baseline for the experimental data.

Eleven different sutures were examined in each of the rat skulls from both the experimental and wild rat groups. The sutures included the premaxillomaxillary (right and left), frontonasal, frontopremaxillary (right and left), frontomaxillary, interfrontal, frontoparietal, interparietal, parietosupraoccipital and the occipitosupraoccipital (Figure 1). These sutures were traced and then digitized on the computer to determine their complexity. The digitization involved measuring both the length and the distance of a suture. These numbers were converted into a ratio of length over distance which gave a numerical notation of complexity.

RESULTS

After quantifying the degrees of complexity among the experimental and wild rat sutures through digitization, the results showed that in the facial suture interdigitation did vary with dietary consistency (Figure 2). On the other hand, the braincase sutures did not show apparent changes associated with the changing diets (Figure 3). These results revealed that complexity did not increase according to diet among the different sutures as we had hypothesized. The sutures that numerically proved to be significantly different from the wild rat groups were random sutures not found in any particular region of the skull. These sutures included the left premaxillomaxillary, the frontonasal, the frontoparietal, the interparietal and the occipitosupraoccipital. The other six sutures were not significantly different than the wild rat data. A significant difference was determined by an average difference that was greater than 0.5 among the experimental and wild rat groups.

CONCLUSIONS

An important issue that has been addressed in this paper is the issue concerning sutural morphology. As stated earlier, although some characteristics of sutures are genetically programmed (i.e. intrinsic), it has been shown in rats that sutural morphology ranging from simple straightline sutures to highly interdigitated sutures (Herring, 1972)

are determined by extrinsic forces acting upon these sutures. In other words, the forces produced during biting and gnawing may be responsible for modifying the development and complexity (interdigitation) of some of the cranial sutures in the anterior portion of the skull (Massler and Schour, 1951; Moss, 1958, 1961; Moss and Young, 1960; Jaslow, 1989).

The results from this preliminary study indicate that some of the sutures in the rat's skull could be induced during development to show variation in complexity associated with changes in diet. The data is very interesting in that it is opposite from what we had expected. We expected as the diets got harder the sutures would become more complex, but instead we saw that the sutures in the facial region became less complex as the diet got harder. Many studies have shown that when rats are fed soft diets there are several very noticeable changes in the skull's structure (Moss, 1961; Moss and Young, 1960). It has been shown that the cranial bones are thinner, the skulls are narrower and the muscles become smaller due to atrophy. These changes may have caused different and unpredicted patterns and force to the skull. The results are rather inconclusive, but this only opens the door for a great deal more research of cranial suture development in white lab rats.

REFERENCES

- Jaslow, C. R. (1989). "Sexual Dimorphism of Cranial Suture Complexity in Wild Sheep (*Ovis orientalis*)." *Zool. J. Linn. Soc.* 95: 273-284.
- Jaslow, C. R. (1990). "Mechanical Properties of Cranial Sutures." *J. Biomechanics.* 23: 313-321.
- Massler, M. and I. Schour. (1951). "The growth Pattern of the Cranial Vault in the Albino Rat as Measures by Vital Staining with Alizarine Red 'S'." *Anat. Rec.* 110: 83-101.
- Moss, M. L. (1958). "Rotations of the Cranial Components in the Growing Rat and their Experimental Alteration." *Acta Anatomica.* 32: 65-86.
- Moss, M. L. and R. W. Young. (1960). "A Functional Approach to Craniology." *American Journal of Physical Anthropology.* 18: 281-292.
- Moss, M. L. (1961). "Extrinsic Determination of Sutural Area Morphology in the Rat Calvaria." *Acta Anatomica.* 44: 262-272.
- Oudhof, H. A. J. (1982). "Sutural Growth." *Acta Anatomica.* 112: 58-68.

Table. Rat Diets

GROUP	DIETS
1	LIQUID DIET WITH CLIPPED INCISORS
2	LIQUID DIET ONLY
3	SOFT FOOD
4	SOFT FOOD WITH HARD PARTICLES
5	HARD FOOD
6	HARD FOOD WITH GNAWING MATERIALS

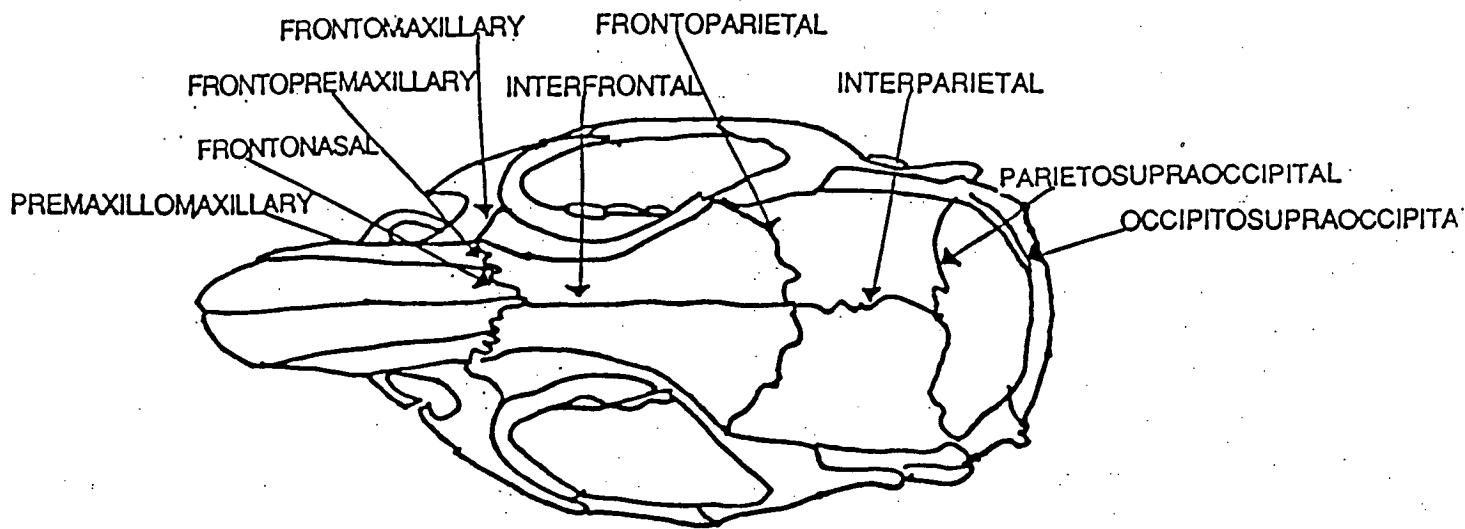


Figure 1. Sutures

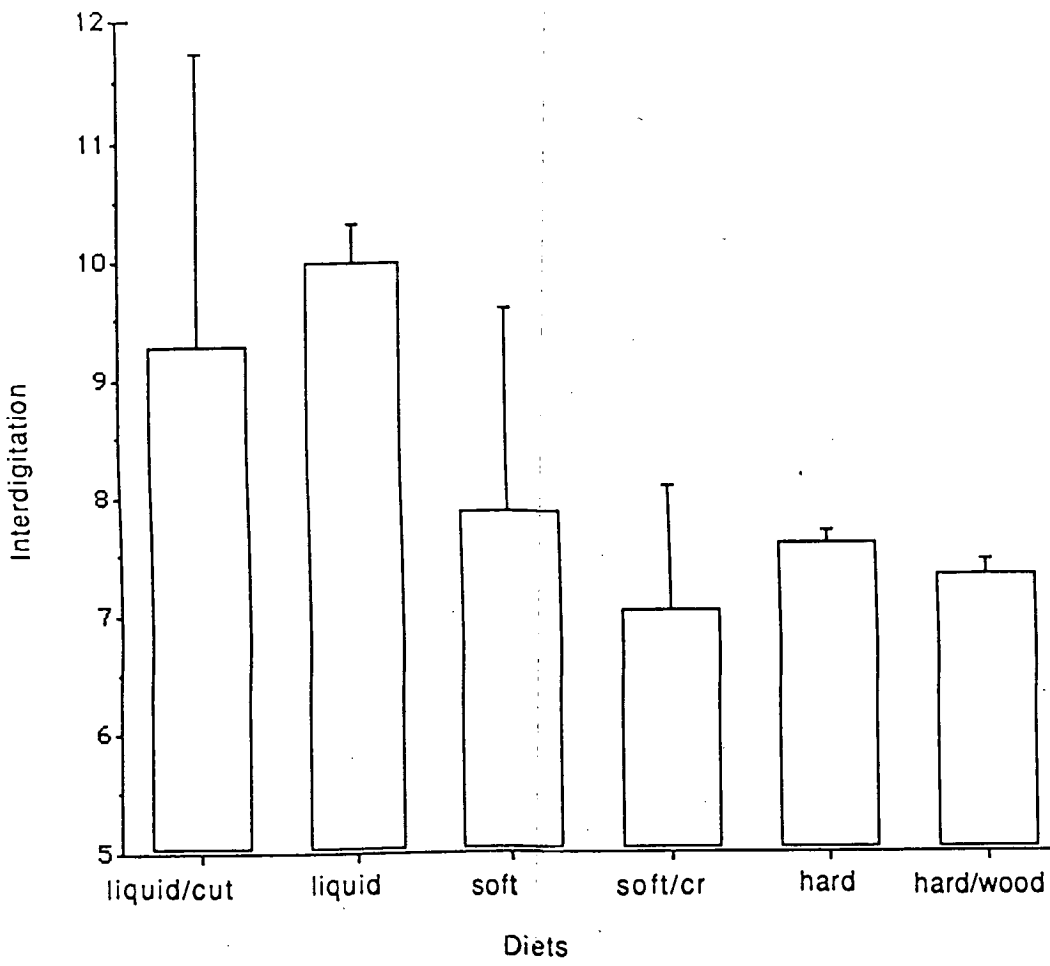


Figure 2. Interdigitation of the fronto-premaxillary suture

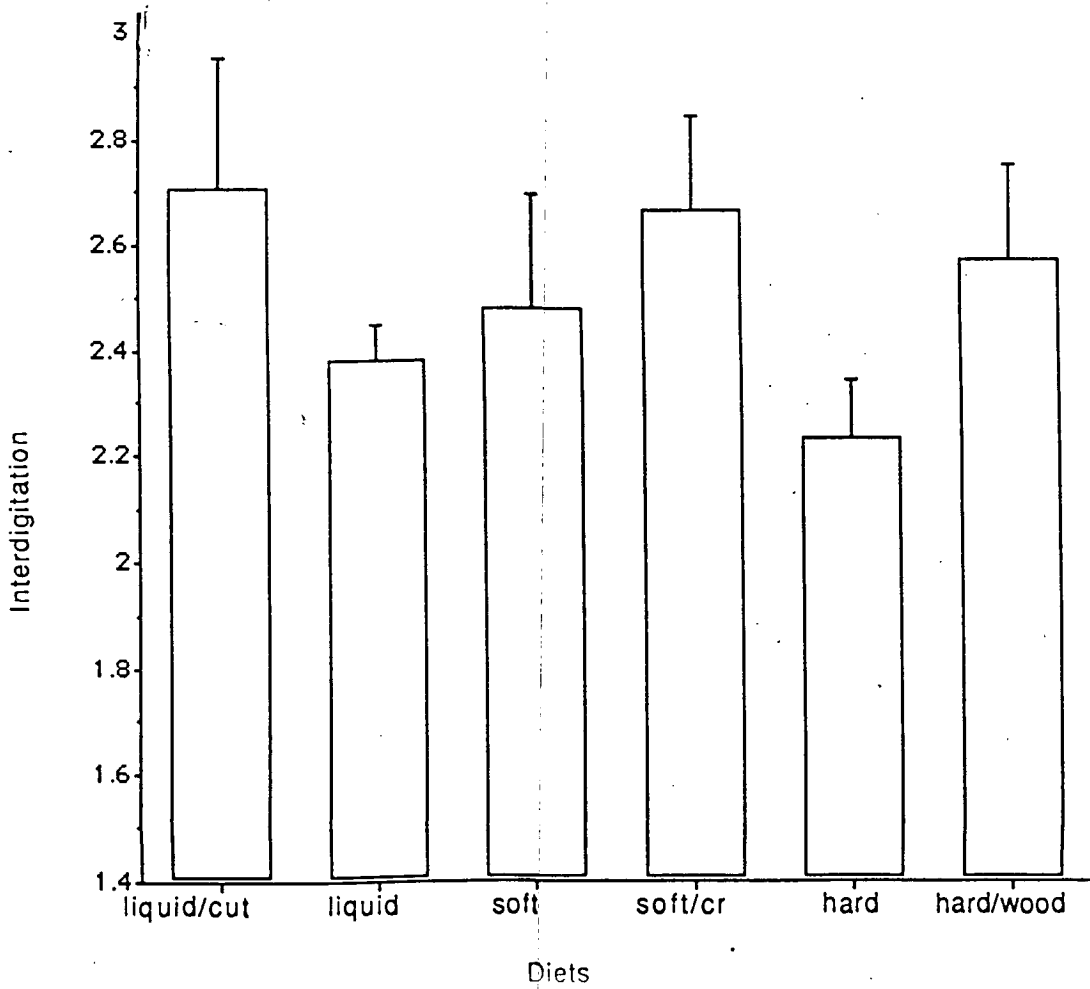


Figure 3. Interdigitation of the occipito-supraoccipital suture

THE BIOLOGICAL ACTIVITY OF TWO CHLORAMPHENICOL DERIVATIVES

KATHY L. WHEELER

ABSTRACT

The goal of this research was to design a new antibiotic, based on chloramphenicol, which would not show the toxic effect that chloramphenicol displays in some cases. Evidence in the literature indicates that the dichloromethyl group of chloramphenicol may contribute to the toxic effect. A chloromethyl ketone has been reported to react with the indigenous sulfhydryl groups that are essential for biological functions. Two new antibiotics were synthesized, and the antibiotic activity of one was similar to chloramphenicol.

From model reactions, however, it appears that the dichloro group in chloramphenicol is relatively unreactive. Therefore, we conclude that the toxic effect of chloramphenicol is not due to the reactivity of the dichloro group.

INTRODUCTION

Why chloramphenicol (CAP) (Figure 1) gives a toxic response in some people is a question that has been asked for many years but has not yet been answered. Yunis (1990) believes that the nitro group of CAP contributes to bone marrow toxicity known as aplastic anemia. His belief is based on the fact that the nitro reduction product, NO-CAP, is much more toxic than the parent compound. Eyer (1984) has shown, however, that most of the NO-CAP formed by microorganisms in the intestine or produced in the liver will be degraded in blood before reaching the bone marrow. This information leads one to investigate other possibilities.

According to reports from two groups, the reactivity of chloromethyl ketones toward indigenous sulfhydryl groups may play an important role in their being toxic. The major effect of chloromethyl ketones in *E. coli* is inhibition of growth, RNA synthesis, and protein synthesis. This effect is the result of the reaction of the chloromethyl ketone with glutathione (GSH) (Rossman, 1974). The chloromethyl ketones are more reactive than the comparable alkyl chlorides by a factor of 35,000 (Bordwell and Brannen, Jr., 1964). This reaction rate is fast enough to allow the chloromethyl ketones to effectively react with the -SH in the body to inhibit O_2^- production, an effect documented by Tsan (1983) in a study of human neutrophils. The broad spectrum antibiotic CAP has a dichloromethyl ketone structure that is expected to be at least as highly reactive as the chloromethyl ketone structure. It is our hypothesis that the dichloromethyl ketone of CAP contributes to its toxicity. This possibility has not previously been investigated.

To reach our goal of lowering the toxicity of CAP while retaining its biological activity, two derivatives of CAP that do not react with RSH were synthesized. These compounds substituted -CN and -phenyl for the -Cl₂ in the parent compound. The structures are illustrated at the end of the paper. The relative antibiotic activity of the two derivatives toward *Proteus mirabilis*, *Salmonella typhimurium*, and *Staphylococcus aureus* were obtained. A model reaction of the reactivity of the dichloro moiety of CAP was investigated.

MATERIALS AND METHODS

Chloramphenicol and its d-Base were obtained from Sigma Chemicals, St. Louis, MO.

The synthesis of CN-AP (Figure 2) involved stirring equimolar amounts of CAP-base with methyl cyanoacetate in ethanol for six days at a temperature of 22 C. The reaction progress was followed with thin layer chromatography on silica gel using ethyl acetate as the solvent. The product was a colorless, crystalline substance with a melting point of 125-127 C. These crystals were shown to be pure by thin-layer chromatography (TLC). Nuclear magnetic resonance (NMR) spectral data supported the assigned structure. The ^{13}C NMR of CN-AP contained the peaks of CAP-base plus a peak at 206 ppm ($-\text{CO}-\text{CH}_2\text{CN}$), 118 ppm ($-\text{CO}-\text{CH}_2-\text{CN}$), and 30 ppm ($-\text{CO}-\text{CH}_2-\text{CN}$).

The phenyl derivative (P-AP) (Figure 3) was made by dissolving CAP-base in methylene chloride and pyridine. After the base was fully dissolved, benzoyl chloride was added to the reaction flask. The organic layer of the reaction mixture was extracted. After concentrating the organic layer, a white solid precipitated. The phenyl derivative was purified by recrystallization from CH_2Cl_2 . The melting point of P-AP is 169-170 C. The structure of this compound was verified by ^1H NMR. The spectrum of the P-AP compound in DMSO and D_2O showed the additional aromatic peaks at 7.6-7.7 ppm for the benzoyl derivative. The protons that absorb at 2.5 ppm on the spectrum of the CAP-base are due to NH_2 . This group should not be present in P-AP, and the disappearance of this absorbance is good evidence that the product is what was expected.

The biological activity of the antibiotics was determined by following the absorbance at 686 nm of bacterial broths on a Spectronic 20 equipped with a Milton Roy wide-range phototube with filter. Tryptic Soy broth was prepared as a growth medium for the bacteria according to the instructions on the label. Pathogenic bacteria, *Proteus mirabilis* (gram -), *Salmonella typhimurium* (gram -), and *Staphylococcus aureus* (gram +), were transferred to slats and incubated for two days. Broths of the bacteria were then made. Aqueous solutions of 1 mg/mL CAP, 1 mg/mL CN-AP, and 0.4 mg/mL P-AP were sterilized with a 2.2μ sterile filter. The antibiotic solution was added to sterile growth medium in sterile cuvettes. All test tubes were then inoculated with the bacteria.

Figures 4, 5 and 6 show the results of the experiments. Each experiment used two controls. The negative control contained no antibiotic. The positive control contained chloramphenicol. Each absorbance determination was done in triplicate. The results were averaged for plotting.

In order to investigate the premise of the research, the high reactivity of dichloro compounds, an effort was made to react a dichloro compound with a free amine and to follow this reaction with gas chromatography (GC). 2,2-Dichloroacetamide (39.1 mmol) was reacted with an excess of butyl amine (195.4 mmol) in ethanol (100mL). These reagents were allowed to stir for several hours at 22 C. Anisole was added as an internal standard for the GC experiments. The GC experiments were inconclusive. Several drops of 0.1M AgNO_3 were added to the reaction mixture. There was some cloudiness, but it did not appear to be AgCl . Ammonia dissolves AgCl . The cloudiness did not disappear when ammonia was added which suggests that the cloudiness was caused by an organic compound that is not soluble in the aqueous solution of AgNO_3 .

RESULTS

The first experiment (Figure 4) showed that CN-AP was almost as effective as chloramphenicol at inhibiting *Proteus mirabilis* growth. P-AP was as not effective at inhibiting the growth of this bacterium.

The second experiment (Figure 5) showed the high activity of CN-AP toward *Salmonella typhimurium*. Again, P-AP was not as effective.

The third experiment (Figure 6) showed similar results. CN-AP was again highly active against *Staphylococcus aureus*; although, neither CN-AP nor CAP was as effective as in other experiments. As seen previously, P-AP was not active as an antibiotic.

The two model reactions (Figures 7 and 8) were used to determine the reactivity of the chloro groups in chloramphenicol. 2,2-Dichloroacetamide was used as a model for chloramphenicol, and n-butyl-amine was used as the model for the intrinsic reactive biochemicals. In the first reaction, the products were analyzed by gas chromatography. No change in the composition of the reaction mixture was observed indicating that no reaction occurred.

In the second reaction, silver nitrate was used to determine if chloride ions were present. We found no evidence for the formation of silver chloride which indicates that no reaction occurred in this model system.

CONCLUSIONS

There are two hypotheses on the inactivity of P-AP. The bulk of the phenyl group might cause steric interference and might not allow the reactions that must take place in order to kill the bacteria. A second possibility is that the concentration of P-AP was too low. Due to solubility problems, the concentration of P-AP was 40% that of CAP and CN-AP. This could have profoundly affected its growth-inhibiting abilities.

Although one of the compounds is an effective antibiotic, there is no evidence to suggest that this compound will be any less toxic than chloramphenicol.

REFERENCES

- Bordwell, F.G. and W.T. Brannen, Jr. (1964). "The Effect of Carbonyl and Related Groups on the Reactivity of Halides in SN2 Reactions." *Journal of the American Chemical Society*. 86:4645-4648.
- Eyer, P., E. Lierheimer and M. Schneller. (1984). "Reactions of Nitroso-chloramphenicol in Blood." *Biochemical Pharmacology*. 33:2299-2308.
- Rossmann, Toby *et al.* (1974). "Inhibition of Macromolecular Synthesis in *Escheria coli* by Protease Inhibitors." *The Journal of Biological Chemistry*. 249:3412-3417.
- Tsan, Min-Fu. (1983). "Inhibition of Neutrophil Sulfhydryl Groups by Chloromethyl Ketones: A Mechanism for their Inhibition of Superoxide Production." *Biochemical and Biophysical Research Communications*. 671-677.
- Yunis, A.A., M.D., FACP *et al.* (1990). "Interaction of Chloramphenicol and Metabolites with Colony Stimulating Factors: Possible Role in Chloramphenicol-induced Bone Marrow Injury." *The American Journal of the Medical Sciences* 300:350-353.

ACKNOWLEDGMENT

We would like to thank Dr. Hill of the biology department of Rhodes College for his help in this project. His assistance in selecting a method of studying biological activity as well as in choosing the bacteria with which to work was needed and appreciated.

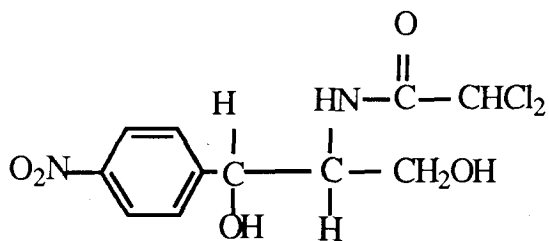


Figure 1. Chloramphenicol (CAP)

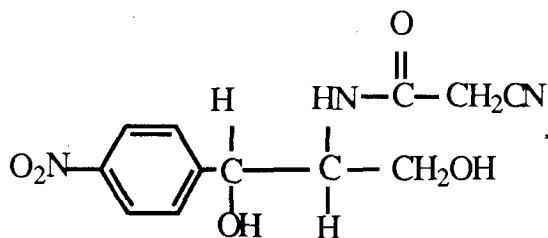


Figure 2. CN derivative (CN-AP)

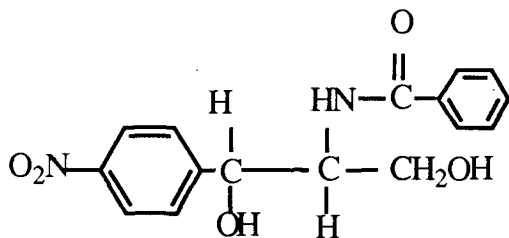


Figure 3. Phenyl derivative (P-AP)

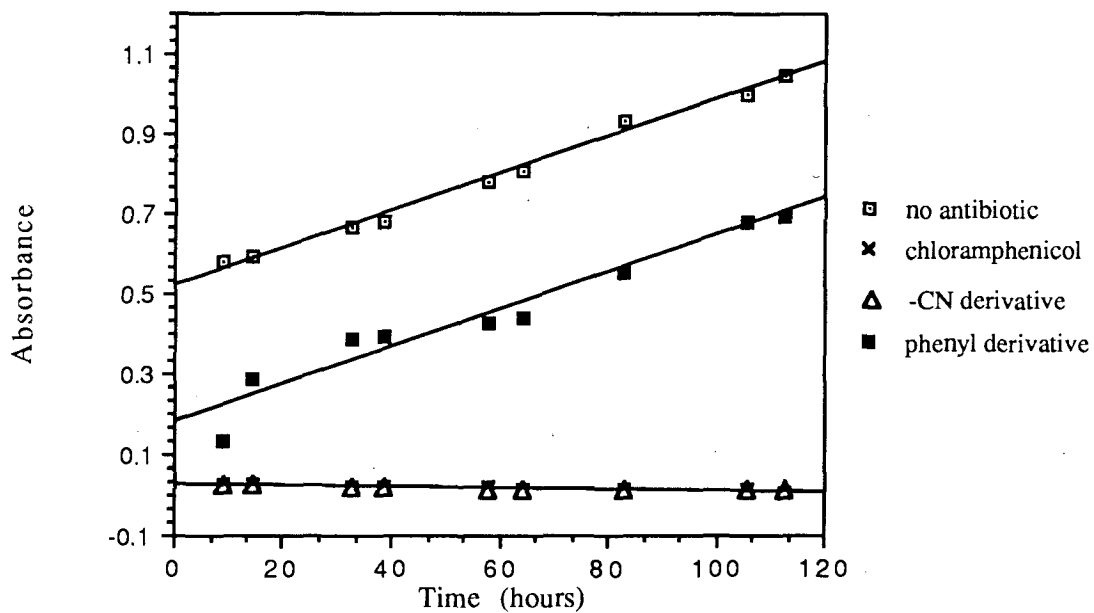


Figure 4. Study on *Salmonella typhimurium*

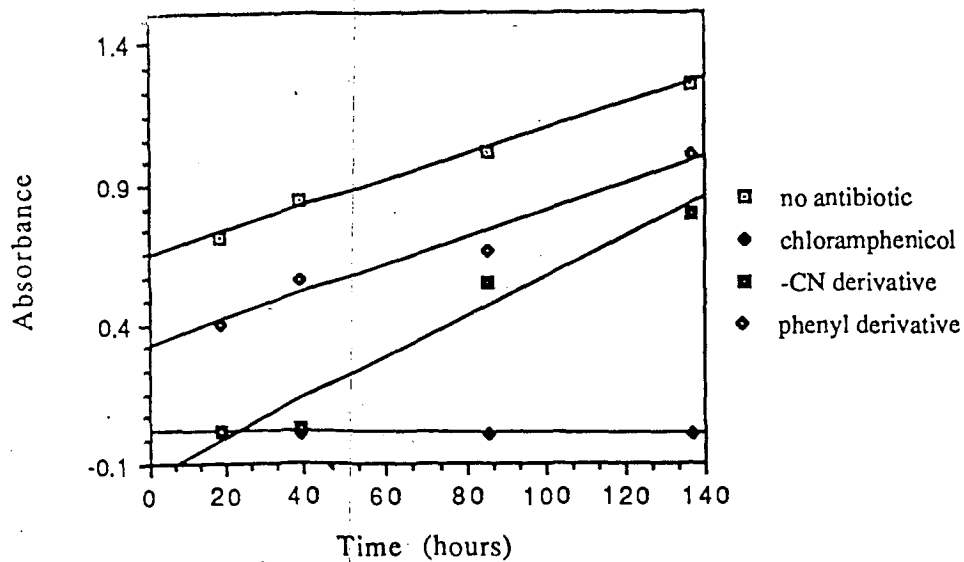


Figure 5. Study on *Proteus mirabilis*

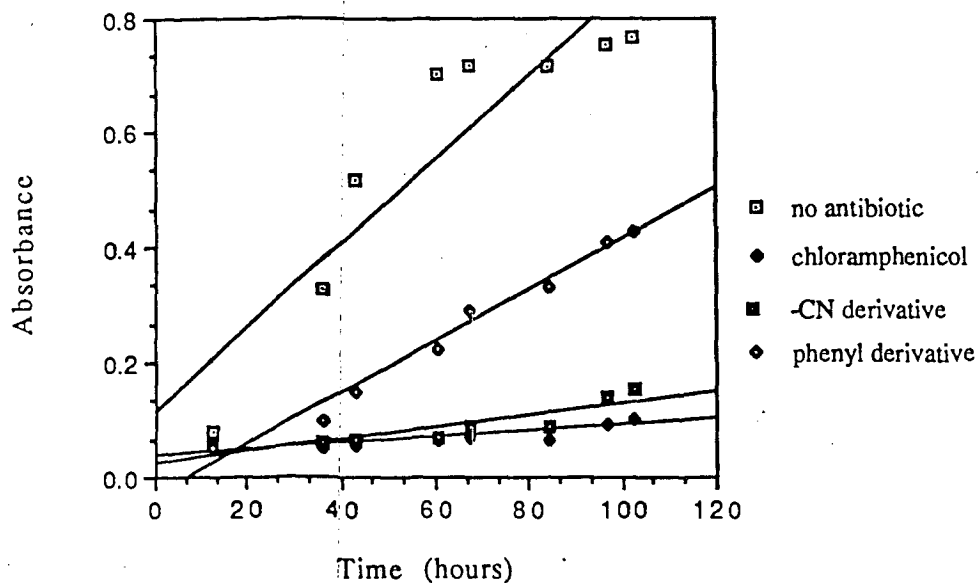


Figure 6. Study on *Staphylococcus aureus*

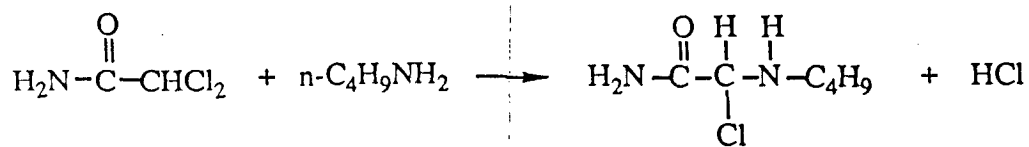


Figure 7. Assay for reactivity of 2,2-Dichloroacetamide in the model system

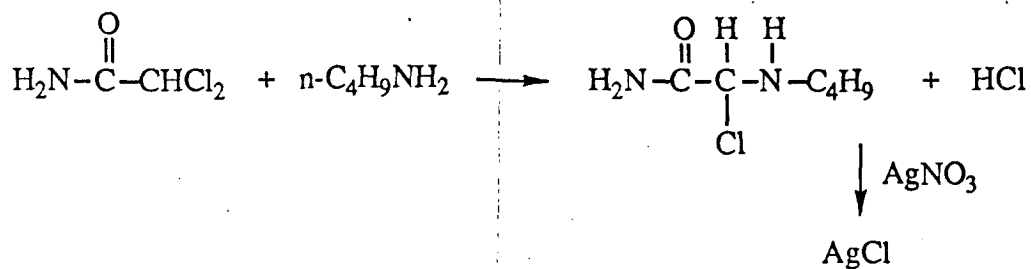


Figure 8. Assay for free chloride ions in the model system

SOLAR Ca K IRRADIANCE VARIATIONS THROUGH ONE SOLAR ROTATION

TREY WHITE

Done in partial fulfillment of the requirements for the Bachelor of Science Degree with Honors in Physics

ABSTRACT

Measurement of the doubly ionized K line calcium in the solar spectrum (Ca K) offers a good "proxy" measurement of the UV output of the sun. Measurements of this line were made at Rhodes College between February 18, 1992, and March 16, 1992, using the Rhodes College Czerny-Turner spectrograph with a CCD detector. These measurements were compared with Ca K data from Sac Peak and UV data from SOLSTICE. These comparisons highlighted possible problems with scattered light and tracking of the sun. Memphis weather conditions did not prove to be a great hindrance.

INTRODUCTION

The following describes the motivation, goals, preparation, procedure, and data analysis for an experiment in the field of solar physics. The experiment involved the measurement of the intensity of a portion of the sun's spectrum and the study of the daily variation of that intensity over an entire rotation of the sun. The portion of the spectrum of interest was that which includes a wavelength of light emitted by singly ionized calcium in the chromosphere, the outermost layer of the sun. The detector used in the experiment was a "charge coupled device," or "CCD." The experiment has been performed as an honors project earning a total of six hours of academic credit and partially fulfilling the requirements for the Bachelor of Science Degree with Honors in Physics.

MOTIVATION

The amount of radiation coming from the sun varies over the 27 day rotation of the sun and the 22 year cycle of solar magnetic activity. This variable radiation, particularly ultraviolet radiation, reacts strongly with the upper atmosphere of the earth. Concerns about ozone layer depletion and general concerns about our climate have placed greater importance on our understanding the upper atmosphere of the earth and, thus, the variable radiation coming from the sun.

These ideas are discussed in the 1989 report *A Research Plan For the 1990's On Solar Irradiance Variation* from the National Science Foundation (NSF). In the Executive Summary, the report states, "Measurement and understanding of the sun's variable radiative outputs poses one of the most important problems in solar research," citing its "direct impact on research in climate variation and stratospheric chemistry, both topics of intense current concern."

In considering specifically the problem of variability of the earth's ozone layer, the area of interest in the spectrum of solar radiation is the ultraviolet (UV). Since solar UV radiation is absorbed by the ozone in the atmosphere, the radiation in this area of the spectrum is prevented from reaching the surface of the earth where it would otherwise be detectable by ground-based telescopes and spectrographs.

Though ground-based measurement of this important UV radiation is impossible, "proxy" measurements may be taken at other wavelengths which tend to

be emitted from the sun in amounts proportional to the UV emissions. One such "proxy" measurement is that of the radiation emitted by ionized calcium at a wavelength of about 393 nm,¹ known as the "calcium K line," or "Ca K." The variability in Ca K radiation measured over the face of the sun (full-disc) has been found to agree to within 5% of the variation in the UV.²

Because of this close correlation, measurements of Ca K have been made over complete solar rotations and substantial parts of solar cycles and used to analyze and model UV activity over these time scales, scales too long for extended direct measurement of the UV by satellites. Regular measurements of the full-disc Ca K emission have been obtained, weather permitting, since 1975. As of 1989, measurements were being made at the Kitt Peak, Sacramento Peak, and Lowell Observatories.³

The NSF report mentioned earlier emphasizes the importance of these Ca K measurements, and recommends that additional sites be equipped to make these measurements so that ongoing *daily* measurements may be obtained to provide the necessary careful cross-calibration of the measurement data and the redundancy "... necessary to minimize gaps caused by poor weather or equipment malfunction at individual sites."⁴ With daily measurements over the time scales of solar rotations and solar cycles, the report asserts that greater understanding and more accurate modeling of solar UV emission will result.⁵

PROJECT GOALS

The primary goal of the honors project described here was to obtain daily measurement of the full-disc Ca K emission, weather permitting, over a single solar rotation of 27 days. The measured data were then to be analyzed for variability, resulting in a map of how the Ca K emission varied over the solar rotation. This result was then to be compared to results from other sites and to satellite UV data.

The comparison with results from other sites satisfied a secondary goal of this project, to test the suitability of Rhodes College as an additional site for the ongoing daily measurement of Ca K, as recommended in the NSF report. The physics department is currently working on a joint venture with the Laboratory for Atmospheric and Space Physics at the University of Colorado, a venture in which Rhodes College may receive one of a number of identical instruments used to measure full-disc Ca K across the country.

A tertiary and final goal was to compare the effectiveness of the facilities and equipment used for this honors project with the instruments to be used in the joint venture. This comparison was to determine the feasibility of using these facilities as a backup for the joint-venture apparatus and as a source for cross calibration.

OVERVIEW OF THE EXPERIMENTAL SETUP AND PROCEDURE

The experiment employed the following major components: the heliostat on the sixth floor of Rhodes Tower, the 3.4 meter Czerny-Turner spectrograph, a CCD detector, a personal computer (PC), and Sun workstations in the math/computer science department and physics department. The purpose of the heliostat was to direct solar radiation into the spectrograph room. This beam was sent through a spectral filter to remove unwanted wavelengths of light and was directed to the entrance slit of the spectrograph. Finally, after the light was dispersed by the diffraction grating within the spectrograph, a CCD detector created a digital image of the spectrum that was saved on the PC. From the PC, the image data were moved to a workstation, where they were calibrated and analyzed with a standard software

package used in scientific image processing called IRAF.

The region of the sun's spectrum covered in the image data was very close to the center of the Ca K line. Within the nearly continuous visible spectrum of the sun, a few dark bands of absorption exist. The Ca K line appears as one such absorption band as a result of the calcium present in the relatively cool upper regions of the chromosphere. During periods of high solar activity, however, a Ca K *emission* band appears dimly in the center of this Ca K *absorption* band. It is the intensity of this emission band that was measured. This intensity was then compared with the constant brightness of the continuum spectrum of the sun to determine the variability in the band, and, thus, the variability in solar activity.

EXPERIMENTAL PREPARATION

Before any measurements could be taken, the major components of the experimental setup had to be aligned, calibrated, and tested. In some cases, the results of this testing revealed a necessity for modification and repair. The major components of the setup were the heliostat, the Czerny-Turner spectrograph and its CCD detector, and the optics between these two components.

The first of these components to be tested, and the component upon which the others were most dependent, was the heliostat. Mounted on the porch atop Rhodes Tower, the heliostat was designed to track the sun, thus directing an unmoving beam of sunlight into the building, where the beam was to be reflected down into the Czerny-Turner spectrograph room on the first floor. To accomplish this task, the heliostat relies on a primary mirror rotating about the polar axis (Figure 1). Further along the polar axis is a stationary secondary mirror. By rotating at the same rate as the earth, the primary mirror maintains a beam of sunlight squarely on the secondary mirror. The secondary mirror may then be pointed so as to direct this beam where desired. In the case of the measurement of Ca K, it was necessary that the beam remain stationary for half an hour over a distance of almost 100 feet: down through the physics building, across the Czerny-Turner spectrograph lab, and through various optics. This requirement put strict limits on the error in alignment and rate of rotation of the heliostat. Numerous adjustments were made to the alignment in order to have the axis of rotation adequately close to true North and centered on the secondary mirror, adjustments including use of alignment lasers and specially mounted telescopes directed toward Polaris, the North Star. Also, the rotation driving motor was repaired and cleaned so that it would drive close enough to the rate of rotation of the earth for adequate tracking. Despite the sustained efforts of Dr. Jack Streete, department technician Joe Crawford, and the author, the heliostat was not in adequate working order until late January of this year. Thus, the many aspects of preparation relying on a working heliostat could not be performed until this time.

Luckily, much of the preparation of the Czerny-Turner spectrograph and its CCD detector did not rely on a working heliostat, so this preparation was performed concurrently. The spectrograph (Figure 2) had been re-aligned in the summer by its designer, Dr. Ed Dorman, so the first steps were to mount the CCD and determine the diffracting order in which the spectrograph would be used.

A diffraction grating, like the one in the Czerny-Turner spectrograph at Rhodes, produces multiple spectra, each at different angles. Normal reflection represents the "zero order," where no light dispersion occurs. The first dispersed spectrum away from this zero order is the "first order," the next is the "second order," and so on. The higher the order, the more the light is dispersed. Unfortunately, the more the light is dispersed, the more the energy is dispersed, making the spectra more difficult to detect. Thus, with a diffraction grating designed for work in multiple orders, such as that found in the Czerny-Turner spectrograph, the most

desirable order from which to take data is the lowest one that provides adequate dispersion of the light. To properly resolve the Ca K line, a wavelength resolution of at least 35 mÅ (3.5×10^{-3} nm) is required.⁶ Routine spectroscopic calculations using the Czerny-Turner spectrograph and Lynxx CCD detector specifications⁷ showed that using the third order would result in a resolution of about 22 mÅ per pixel on the detector, where second order would yield 33 mÅ per pixel. To stay safely within the required resolution, third order was selected.

The remaining preparation of the spectrograph involved mounting and calibrating the CCD. Mounting proved to be relatively simple, for the detector was shaped similarly to the housing of the exit slit of the spectrograph. Thus, with minimal machining, the CCD was attached to the housing after the exit slit assembly was removed. Once the electronics and software were in place to run the CCD, test spectra were made using laboratory light sources. First, the CCD was focused by comparing subsequent exposures of the bright and easily distinguishable 546.06 nm line of the mercury spectrum. From these exposures, it was obvious that the entrance slit was too wide to achieve the desired 35 mÅ resolution, even at the smallest obtainable slit width. This problem was solved, however, by adjusting the entrance slit assembly so that smaller widths were possible. The final physical preparation of the spectrograph was to allow for accurate small-angle rotation of the diffraction grating. Precise small-angle rotations would be necessary to properly position the spectral areas of interest on the tiny face of the CCD detector, a square face only 2.64 mm on a side.⁸ An optical comparitor was mounted atop the spectrograph, and the rotating arm controlling the grating position was attached to it. By turning the large comparitor screw knob, the grating arm was moved very slightly, allowing for precise small angle rotations of the grating.

The final preparation of the spectrograph was calibrating the CCD and the spectrograph wavelength position. First, the Ca K wavelength, 393.35 nm, had to be located within the third order diffraction spectrum. Luckily, 393.35 nm in third order was at the same position as 590.0 nm in second order, a position near the easily distinguishable 589.6 nm line of sodium. Since the 192 columns of the CCD detector covered a second order range of approximately 0.6 nm, placing the second order 589.6 nm line at the proper edge of the CCD would have placed the 590.0 nm position just past the center. Thus, a sodium source was used in second order to find the third order position of Ca K to within the width of the detector. The actual Ca K absorption line was placed exactly using direct exposures of the sun, since the unique and easily recognizable Ca K spectrum was within the image area.

To measure the daily change in the Ca K level, the spectra needed to be compared with an area of the solar spectrum known to be relatively constant. Originally, the constant area to be used was at 395.4 nm. Therefore, 395.4 nm in third order also needed to be located. Again, its second order partner was used. 395.4 nm in third order overlaps 593.1 nm in second order, and nitrogen has a strong emission line very near 593.1 nm. Thus, as a sodium source was used to find 393.46 nm, a nitrogen source was used to find 395.4 nm.

The sodium source was used again to make the final calibration of the CCD: to determine the actual wavelength dispersion per column of pixels. The lines of the yellow sodium doublet, 589.6 nm and 589.0 nm, both just fit on the face of the CCD when used in second order. Therefore, each column of pixels represents 31.2 mÅ (0.5974 nm/191.3 columns) in second order, or 20.8 mÅ in third order.

During the taking of spectra with the laboratory sources used in preparation, it became apparent that use of the internal cooler on the CCD detector would be required for the long exposures that were planned for the actual data. The internal cooler was intended to keep the CCD at -30°C, so that internal thermal noise, or "dark current," would be kept to a minimum. Uncooled, the CCD could not make useful

exposures longer than 30 seconds, while it could make over 5 minute exposures when cooled. Unfortunately, the seal on the CCD was broken before delivery from the manufacturer, allowing air into the container. Thus, when the cooler was activated, a film of ice formed on the face of the CCD. The final preparation of the spectrograph for taking data was, therefore, replacing the CCD detector. Unfortunately, this replacement became necessary just as the heliostat became operational, so the actual taking of data was postponed further.

When both the heliostat and spectrograph had become operational, testing of the optics connecting the two began. The most important role of these intervening optics, aside from the obvious direction of light into the spectrograph, was to remove unwanted wavelengths of light. As mentioned earlier, 393.46 nm in third order overlaps 590.0 nm in second order. Though this was beneficial in *finding* 393.46 nm, 590.0 nm had to be removed to *measure* 393.46 nm. Originally, this feat was to be accomplished by a "predisperser". After being reflected by plane mirrors into the spectrograph lab, the sunlight was to be directed through a small prism spectroscope before entering the spectrograph. The spectroscope was set so that the region of the spectrum around 393.46 nm would leave the exit slit of the small spectroscope and enter the Czerny-Turner spectrograph. Unfortunately, when this setup was tested, insufficient energy entered the Czerny-Turner spectrograph to register at the detector. Multiple combinations of focusing lenses and mirrors were used with the small spectroscope in attempts to put more light into the Czerny-Turner spectrograph, but no combination returned adequate results. Eventually, it was determined that the optics within the small spectrograph itself were absorbing or restricting the light around 393.46 nm. Therefore, a different predisperser was required.

A broad-band cut-off filter was selected for the task, a blue filter from Janos Technology Incorporated. The filter transmitted 92% of the light at 393.46 nm but transmitted almost none (less than 0.001%) at 590.0 nm.⁹ Using this filter, the final optical setup was determined (Figure 3). Light from the heliostat hit a plane mirror which reflected it down through the building. Another plane mirror in the basement reflected the light across the room to a third plane mirror. This third mirror reflected the light to a final plane mirror near the entrance slit of the spectrograph, which reflected the light away from the entrance slit onto a focusing mirror. The focusing mirror provided a means of transferring maximum light energy into the spectrograph while assuring that the energy reaching the CCD came from the full solar disc. It accomplished this by reflected the light through the filter and making an image of the second plane mirror at the entrance slit of the Czerny-Turner spectrograph. By imaging this second plane mirror, more energy entered the spectrograph, but the sun was not in focus. Thus, the spectrum was not of one area of the sun, but of the whole solar disc.

EXPERIMENTAL PROCEDURE

The Ca K line was measured each day, weather and time permitting, from February 18 to March 16, resulting in measurements on February 18, 20, 21, 28, and 29 and on March 1, 11, 14, 15, and 16. Days between February 18 and March 1 and between March 11 and March 14 upon which no data was taken were eliminated only because of improper weather conditions. In this case, "improper weather conditions" meant the existence of any clouds at all near the sun during the times of possible measurement, typically one to three hours between 9:30 a.m. and 3:30 p.m. The 9:30 a.m. and 3:30 p.m. limitations were physical limits placed by the heliostat, and the short times of possible measurement were limits placed by the outside commitments of the author. If measurements could had attempted from 9:30 a.m. to 3:30 p.m. each

day, it is likely that four to six more days could have produced successful measurements.

Data for each successful day required the measurement of three components: the Ca K spectrum, a continuum, and the thermal background. Earlier measurements, those from February 18 to March 1, anticipated 395.4 nm to be the continuum value used to calibrate the Ca K measurements. Thus, measurements during that time took separate Ca K and continuum exposures. Afterwards, information from Dr. W. C. Livingston at the National Solar Observatory revealed that the effective continuum could be measured at wavelengths as close as 393.4682 nm, just 0.1 nm from the Ca K line itself.¹⁰ Therefore, adequate continuum data were located within the Ca K exposures themselves, since those exposures covered a 0.4 nm region about the Ca K line. As a result, the data for the remaining days, March 11 to March 16, consisted of only Ca K exposures and thermal background exposures.

From February 18 to March 1, data were taken as follows. First, the CCD cooler was activated, and the CCD was allowed to reach thermal equilibrium. With the heliostat running and aligned with the sun, a short test exposure at 395.4 nm was taken. From the histogram of the test exposure, a proper exposure time was determined. Exposure times, ranging from 135 seconds to 180 seconds, were chosen so that the 395.4 nm images were fully exposed. Once these times were determined, an exposure run was taken. This "run" consisted of five exposures using the same exposure time: one 395.4 nm exposure, two Ca K (393.36 nm) exposures, another 395.4 nm exposure, and a thermal background exposure. After each run, the heliostat was adjusted, if necessary. Three successful runs were taken on February 18, three on February 20, two on February 21, one on February 28, three on February 29, and three on March 1.

After these measurements were taken, it was determined that 393.46 nm could be used as a continuum measurement to compare with Ca K, instead of 395.4 nm.¹¹ The 393.46 nm line had the great advantage of being within the frame of the exposures taken of the Ca K line itself. Therefore, with the use of this line, the grating could remain fixed, and more exposures of Ca K could be taken since no separate continuum exposures would be necessary. Indeed, the 393.46 nm line was used, and measurements from March 11 reflected this change in technique. On March 11, only Ca K (four exposures) and thermal background (two exposures) were measured. Exposure times were lengthened to fully expose the CCD under the smaller irradiance of the Ca K line as compared with 395.4 nm. Unfortunately, these longer times were up to 400 seconds, and the thermal background alone tended to saturate some pixels in such long exposures. These saturated pixels could not be properly corrected, so they were simply eliminated from the data.

To avoid this saturated pixel problem, the procedure was changed once more, and all exposure times were set to 100 seconds. Each run then consisted of six Ca K exposures and a thermal background exposure. These shorter exposures were then added together after the thermal background had been subtracted from each. Two runs using this procedure were taken each day from March 14 to March 16.

DATA ANALYSIS

The first few steps of the data analysis used the PC and the CCD controlling software, while the remaining bulk took place within the environment of IRAF on a workstation. The first step, regardless of the data acquisition procedure, was the subtraction of the thermal background. Thermal background is created within the CCD detector as a result of the thermal energy of the detector itself. Since the rate of background contribution is constant over the time frame of hours, the total thermal background is only a function of exposure time, if the exposures are all taken within

the same day. So, to remove this thermal background from an image, one simply subtracts an image of the thermal background, an image acquired with the same exposure time as the data image, but with the shutter closed. Thus, the first step of the data analysis was the subtraction of these thermal images, taken at the end of each run, from the data images.

Because the exposure times used for the measurements in February and on March 1 were chosen to properly expose 395.4 nm, between 135 seconds and 180 seconds, the Ca K exposures were only partially exposed. Thus, the second step in the data analysis was adding consecutive exposures to create a small number of fully exposed images. Since each run included two consecutive Ca K exposures, these were easily added to produce a single brighter image. Since the March 11 exposures were fully exposed, they did not require adding. The March 14, 15, and 16 exposures, however, at only 100 seconds each, were added in groups of three. All resulting images were then saved in a format readable by IRAF and transported via floppy disk to a workstation.

The first problem of the data analysis attacked within IRAF was that of removing the optical background from the images. Each image was composed of a 192 x 165 array of pixel values. The sun's spectrum was imaged such that the entrance slit of the Czerny-Turner spectrograph was aligned with the columns of the CCD, and such that the spectrum ran horizontally across the 192 rows. The spectrum took up the full width of the CCD and about 2/3 the height. Thus, some darker area existed at the top and bottom of each image. It was hoped that the average value of this dark area in each image represented the value of the optical background. If so, one simply needed to subtract this value from the image to make the zero value of the image equal to the true zero value from which the brightnesses of Ca K and 393.46 nm could be measured.

A test was devised to see if this subtraction of an average value would be accurate. The test compared an image from February 18 and an image from February 28. The comparison first involved averaging each image along the rows to find one average column for each image (Figure 4). The zero level for each image was set such that this column reached zero at the darker top and bottom sections of the image (Figure 5). The average pixel value for each image was then calculated, and each pixel in the images was divided by this average value. This normalized the average pixel value of each image to one. If the zero determination had been accurate, a direct comparison of the two normalized images would have revealed that they almost overlapped one another. Unfortunately, this was not the case. One image varied more greatly than the other about the average pixel value. Specifically, one image had both a higher maximum and lower minimum value than the other (Figure 6). This revealed that the zero levels used for the images were different, and that the method used for determining these zero levels was inaccurate.

Since the true zero level of each image could not be determined independently, the zero level was determined by comparing one day's images with data from an external source, setting that day's zero to the zero of the external data, and then setting the other days' zeroes relative to that day's zero. The first step in this process, the third step of the data analysis (after removing the thermal background and correcting deviant pixels), was aligning the images so that they could be more easily compared. The images were shifted slightly within their data frames so that the lowest point of the Ca K absorption line was centered, or set at column 95. This meant that some of the columns of each image were lost, and others had no data. The shifts were small, however, and the data at the edges of the images were of little interest, so this did not pose a problem. After the images were centered, images from each day were combined by averaging, so that one image represented each day.

A single day was then defined as the standard, and the zero value of that day was set to the zero of other known data. The image for February 18, the first day of

measurement, was chosen as this standard, and the "other known data" came from the Sacramento Peak Observatory in New Mexico (Sac Peak). To set the February 18 image to the Sac Peak data, three values were used: the continuum value at 393.4682 nm, the K3 value, and the K index. The value at 393.4682 nm was the constant value mentioned earlier and was known to be a constant 17.62% of the average solar continuum. The K3 value was the measured intensity of the center of the Ca K absorption line, and was reported by Sac Peak to be 7.44043% on February 18. The K index was a measure of the average value of a 0.1 nm wide section of the solar spectrum centered at the Ca K line. Sac Peak reported a value of 9.73399% on February 18 for this index.

The February 18 image was set to this Sac Peak data in the following way. The ratio of the image value of 393.4682 nm with the average of the image K3 value and K index was set to equal the same ratio of the Sac Peak data. These image values were assumed to be the actual values in the image data minus some unknown background. By assuming this background to be constant over the face of the image, it could be mathematically determined using,

$$\frac{\text{"Sac Peak 393.4682 nm"}}{(\text{"Sac Peak Ca K"} + \text{"Sac Peak K index"})/2} = \frac{\text{"image 393.4682 nm"} - z}{((\text{"image Ca K"} + \text{"image K index"})/2) - z}$$

where z was the unknown background. After calculating this z, it was subtracted from each pixel in the February 18 image.

The zeroes of the other images were then set using the new February 18 image. Since both the K3 value and the K index were expected to change daily — since these values were, in fact, what were intended to be measured — they could not be used in finding the zeroes of the other days. Instead, the ratio used for each image was that of the average value of columns 31 through 41 and 140 through 150 with the average value of columns 65 through 70 and 120 through 125. These columns represented areas of the spectrum outside the center area of the Ca K line, areas of the spectrum known to stay constant over the course of a solar rotation (Figure 7). Columns 31 through 41 were on the short wavelength end of the spectrum, the "left wing", just past the 393.26374 nm absorption line used as a wavelength reference.¹² Columns 140 through 150 were on the long wavelength end, the "right wing", and included the 393.4682 nm continuum line. Columns 65 through 70 and 120 through 125 were just outside the 0.1 nm area around the Ca K line used to calculate the K index. Similarly to the case of February 18, a background value, z, was calculated for each image from these ratios, where z could be found from

$$\frac{\text{"2/18 average of columns 31-41 and 140-150"}}{\text{"2/18 average of columns 65-70 and 120-125"}} = \frac{\text{"average of columns 31-41 and 140-150"} - z}{\text{"average of columns 65-70 and 120-125"} - z}$$

After the proper value of z was subtracted from each image, the images were normalized to their respective values at 393.4682 nm. In other words, each image was divided by the average value of the pixels in column 145 of that image. In this way, the value of each image at 393.4682 nm became "1". These normalized images were then used to determine the daily values of K3 and the K index, which were compared with K3 and K index values from Sac Peak and with direct ultraviolet measurements from the SOLar STellar Irradiance Comparison Experiment (SOLSTICE) aboard the Upper Atmosphere Research Satellite.

RESULTS

The results of the project are shown in three ways: in the values of K3, in values of the K index, and in daily plots of the average of pixels in each column versus the column. These plots show that the procedure for determining the zero values had varying degrees of success (Figures 8a and 8b). With each plot normalized to the image value at 393.4682 nm, or column 145, the right wings of the plots overlapped well. The left wings, however, varied, as did the upper extremities of both left and right wings. Ideal measurements, determinations of zero, and normalizations would have produced plots whose wings overlapped exactly. With these ideal plots, differences seen between plots at the Ca K line could have been attributed solely to differences in solar activity. The deviation in the normalized wings foretold the existence of significant errors in the determinations of K3 and the K index. The calculated values for these were as follows:

<u>Date</u>	<u>K3</u>	<u>K index</u>
2/18	0.07540	0.09691
2/20	0.06486	0.08869
2/21	0.05518	0.08366
2/28	0.08864	0.1066
2/29	0.07004	0.09518
3/1	0.07059	0.09629
3/11	0.08595	0.1029
3/14	0.07059	0.09213
3/15	0.08206	0.09770
3/16	0.07876	0.09823

After determining these values, the values for February 18, 20, 28, and 29 were compared with the February values from Sac Peak¹³ to yield the following results:

<u>Date</u>	<u>Sac Peak K3</u>	<u>K3</u>	<u>% difference</u>
2/18	0.0744043	0.07540	1.34
2/20	0.0736286	0.06486	11.91
2/28	0.0879058	0.08864	0.84
2/29	0.0854095	0.07004	18.00

<u>Date</u>	<u>Sac Peak K index</u>	<u>K index</u>	<u>% difference</u>
2/18	0.0973399	0.09691	0.442
2/20	0.0973282	0.08869	8.875
2/28	0.1056214	0.1066	0.9
2/29	0.1043184	0.09518	8.76

The values from February 18, 20, 21, and 29 were also compared with direct ultra-violet measurements from SOLSTICE.¹⁴ The SOLSTICE values were measurements of the hydrogen Lyman alpha line, and needed to be translated into equivalent K3 and K index values. These equivalent values were calculated by using the values from Sac Peak for February 18 to find a constant of proportionality between Lyman alpha and K3 and between Lyman alpha and the K index. By multiplying the Lyman alpha value of a particular day by the respective constant, an equivalent K3 or K index was found, giving the following results:

<u>Date</u>	<u>Sac Peak K</u>	<u>SOLSTICE Lyman alpha</u>	<u>equivalent K3</u>	<u>%difference</u>
2/18	0.0744043	2.0062	0.074404	—
2/20	0.0736286	1.9823	0.073518	0.1502
2/21	—	2.0354	0.075487	—
2/29	0.0854095	2.2578	0.083735	1.960

<u>Date</u>	<u>Sac Peak K index</u>	<u>SOLSTICE Lyman alpha</u>	<u>equivalent K index</u>	<u>% difference</u>
2/18	0.0973399	2.0062	0.097340	—
2/20	0.0973282	1.9823	0.096178	1.181
2/21	—	2.0354	0.098755	—
2/29	0.1043184	2.2578	0.109545	5.010

An additional day of comparison past those using the Sac Peak data was found from the Lyman alpha data: February 21. The equivalent Lyman alpha K3 value for February 21 was 0.075487, while the measured value for this project was only 0.05518, a difference of 26.90%. The equivalent K index was 0.098755, compared with this project's result of 0.08366, a difference of 15.28%.

These numerical results show what the plots had foretold. Differences between the Ca K data measured at Sac Peak and the actual ultra-violet data measured by SOLSTICE were between 0.15% and 5%, as expected, for the days overlapping with this project's data set. The differences between the project data and SOLSTICE, however, were up to almost 27%. Also, the differences between the Sac Peak data and the project data were up to 18%, almost four times the difference found between the Sac Peak and SOLSTICE data.

CONCLUSIONS

Variations in the Ca K spectra were much greater than expected, and calculations of K3 and the K index compared unfavorably with data from Sac Peak and SOLSTICE, oscillating from values very close to those measured elsewhere to values up to 27% different. Three possible causes for these differences were conjectured: insufficient focus for the spectral resolution required, variable optical background from excessive scattering within the Czerny-Turner spectrograph, and variable light entering the spectrograph because of insufficient tracking by the heliostat.

So far, one of these possible causes has been ruled out: insufficient focus. A test with a helium-neon laser showed the focus to be adequate. The spectral width of the red laser line is 20 mÅ, so a perfectly focused CCD should have recorded the line image as one column wide in second order. The actual exposure produced a width of between one and two columns, giving a spectral resolution of between 21 mÅ and 42 mÅ, meeting the 35 mÅ requirement for Ca K measurement mentioned earlier.

The second possible cause, optical background from scattered light within the spectrograph, is currently being addressed. This scattered light is considered the most probable cause for the irregular optical background found in the data, with irregularity probably the result of the additional effects due to inaccurate heliostat tracking. It is felt that the addition of light baffles and the covering light leaks in the spectrometer housing will substantially reduce this scattered light and improve image quality and spectral resolution significantly (Figure 9). These steps, the addition of baffles and the sealing light leaks, are currently being performed. The results will be included as part of this paper as an addendum.

If the completion of these steps does not reduce stray yield improved images, the tracking of the heliostat will be scrutinized. Another potential improvement is to increase the number of images taken per day. The Sac Peak data represented

averages of over one hundred scans per day.¹⁵ Though numbers such as this would be difficult under this project's conditions (100 s exposures), any increase in number of exposures per day could be helpful.

With the current setup, the facilities for taking Ca K measurements at Rhodes College show themselves to be considerably inferior to those at Sac Peak. If this inferiority is not overcome with the current attempts at improvement, Rhodes College's role in the joint-venture with the University of Colorado could be jeopardized. If the source of the problems is determined to be the Czerny-Turner spectrograph, the joint-venture would not be affected, since a separate specialized spectrometer is to be used. If the source is determined to be the heliostat, however, improvements in tracking capability will need to be implemented before Rhodes College can be a site for the regular Ca K measurements sought in the joint-venture.

Regardless, it appears to be mechanical and optical problems that hamper the taking of Ca K measurements at Rhodes College. Thus, it was physically correctable problems, and not uncontrollable factors such as the weather, that caused experimental problems. The Memphis sky and weather patterns produced an adequate number of days for measurement. The days on which measurements were taken for this project were cloudless, though the only requirement was that no clouds come in front of the sun during actual measurement. If longer times each day could have been devoted to measurement, a considerably larger number of other days could have been used.

WORKS CITED

- 1 J. L. Lean, *et al.*, "Modelling Solar Spectral Irradiance Variations At Ultraviolet Wavelengths," *Solar Irradiance On Active Region Time Scales*, NASA, 1983, p. 254.
- 2 *A Research Plan For the 1990's On Solar Irradiance Variation*, The National Science Foundation, December 13, 1989, p. 2.
- 3 *ibid*, p. 12.
- 4 *ibid*.
- 5 *ibid*, p. 21.
- 6 T. N. Woods, *et al.* "Ground-Based Monitor for the Solar EUV and UV Flux," personal communication, January 29, 1991, p. 1.
- 7 *Lynxx/Lynxx Plus CCD Digital Imaging System User's Manual*, SpectraSource Instruments, Agoura Hills, CA: 1990, p. E-1.
- 8 *ibid*.
- 9 *Precision Optics and Components for Lasers & Scientific Optical Systems*, Janos Technology Inc., Townsend, Vermont: 1989, p. 176.
- 10 W. C. Livingston, personal communication.
- 11 *ibid*.
- 12 W. C. Livingston.
- 13 Timothy Henry, "Ca II K Observations," personal communication, March 10, 1992.
- 14 T. N. Woods, personal communication, March 4, 1992.
- 15 Timothy Henry.

REFERENCES

- A Research Plan For the 1990's On Solar Irradiance Variation.* The National Science Foundation. December 13, 1989.
- Buil, Christian. *CCD Astronomy.* Willmann-Bell, Inc. Richmond, Virginia: 1991.
- CCD Imaging III.* English Electric Valve Company Limited. Chelmsford, England: 1987.
- Henry, Timothy. "Ca II K Observations." Personal communication. March 10, 1992.
- Lean, J. L., et al. "Modelling Solar Spectral Irradiance Variations At Ultraviolet Wavelengths." *Solar Irradiance Variations On Active Region Time Scales.* NASA. 1983.
- Lynxx/Lynxx Plus CCD Digital Imaging System User's Manual.* SpectraSource Instruments. Agoura Hills, CA: 1990.
- Precision Optics and Components for Lasers & Scientific Optical Systems.* Janos Technology Inc. Townsend, Vermont: 1989.
- White, O. R. Personal communication. February 17, 1991.
- White, O. R. "Measurement of the Ca II K Line at KPNO and SPNO." Personal communication. February 8, 1991.
- White, O. R. and W. C. Livingston. "Solar Luminosity Variation. III. Calcium K Variation From Solar Minimum To Maximum In Cycle 21." *The Astrophysical Journal*, 249: 798-816, 1981 October 15.
- Woods, T. N., et al. "Ground-Based Monitor for the Solar EUV and UV Flux." Personal communication. January 29, 1991.

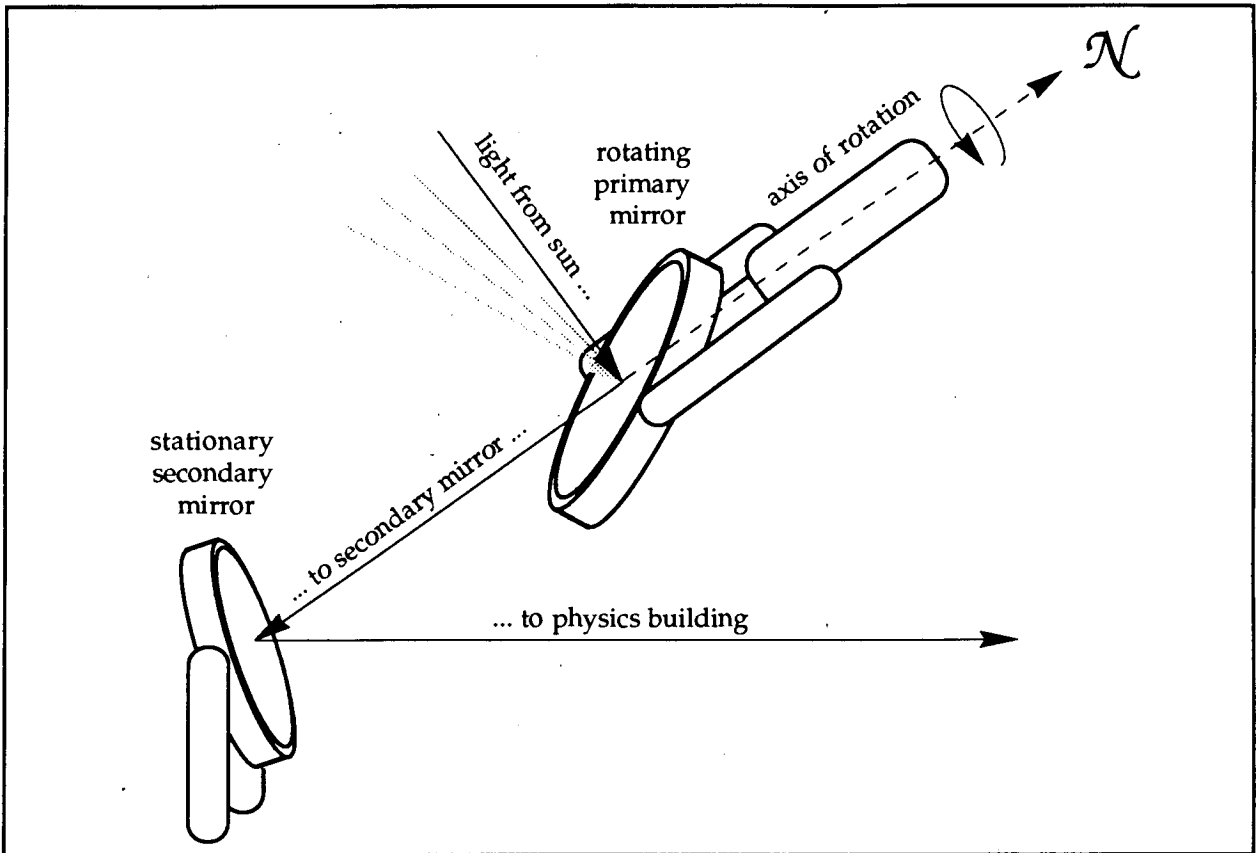


Figure 1. Schematic of a heliostat.

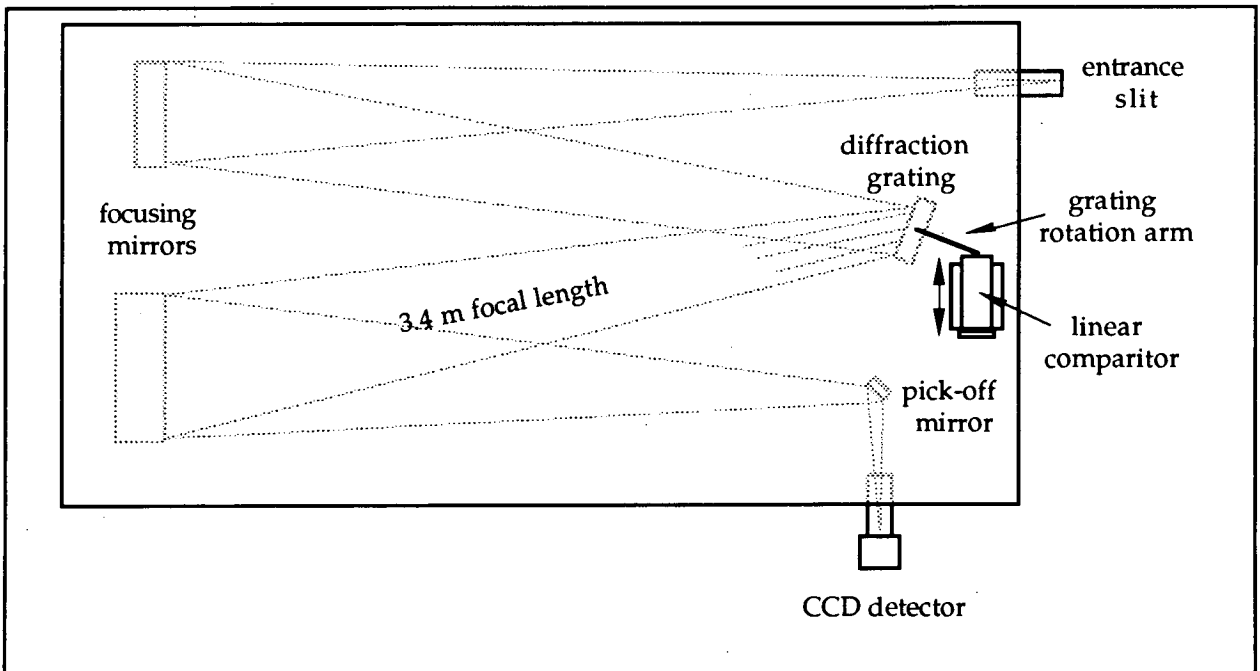


Figure 2. Rhodes College 3.4 m focal length Czerny-Turner spectrograph.

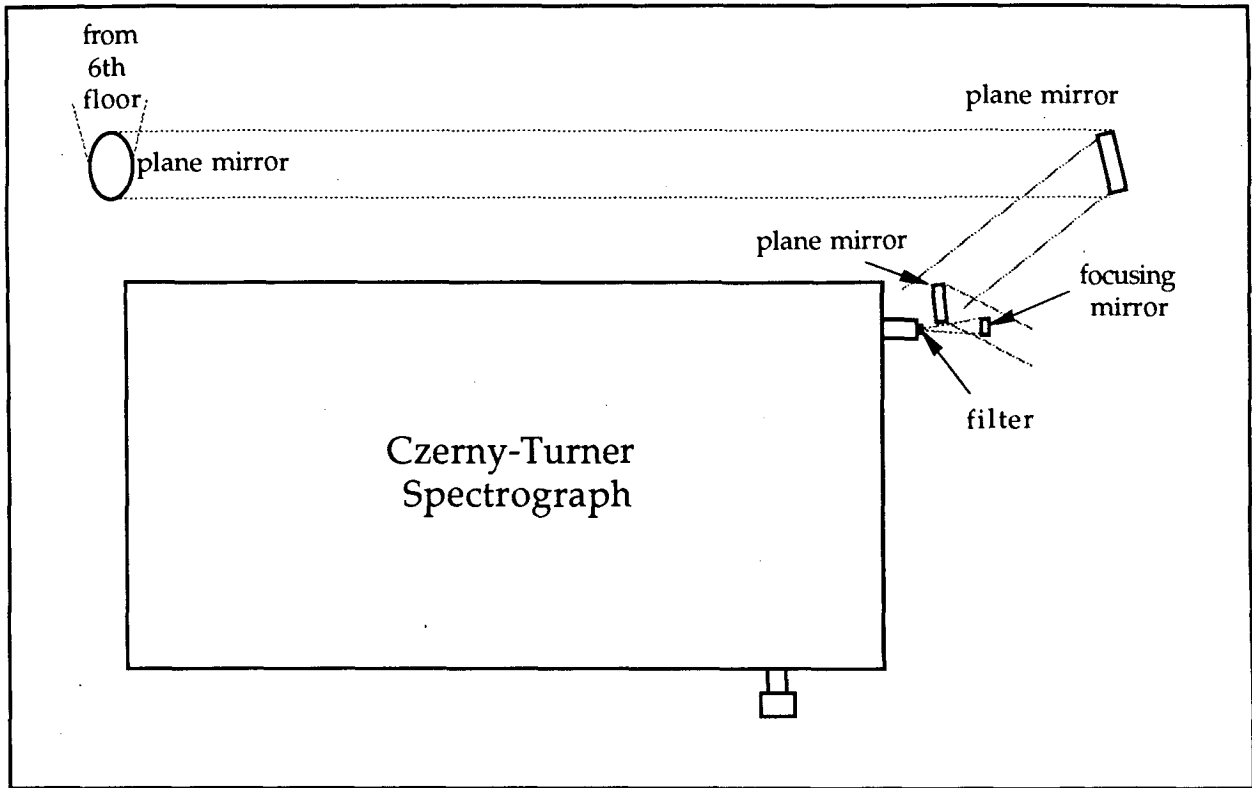


Figure 3. Final optical setup.

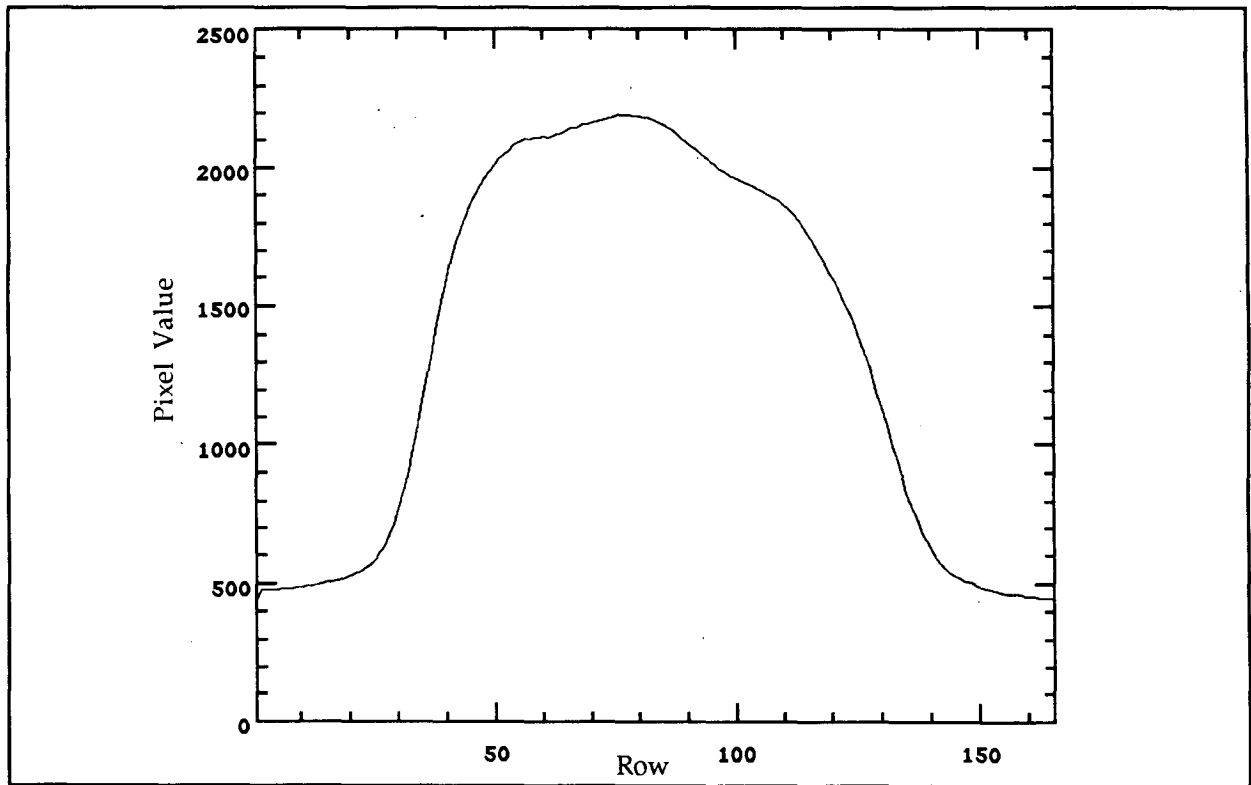


Figure 4. Average Column for 2/18/92.

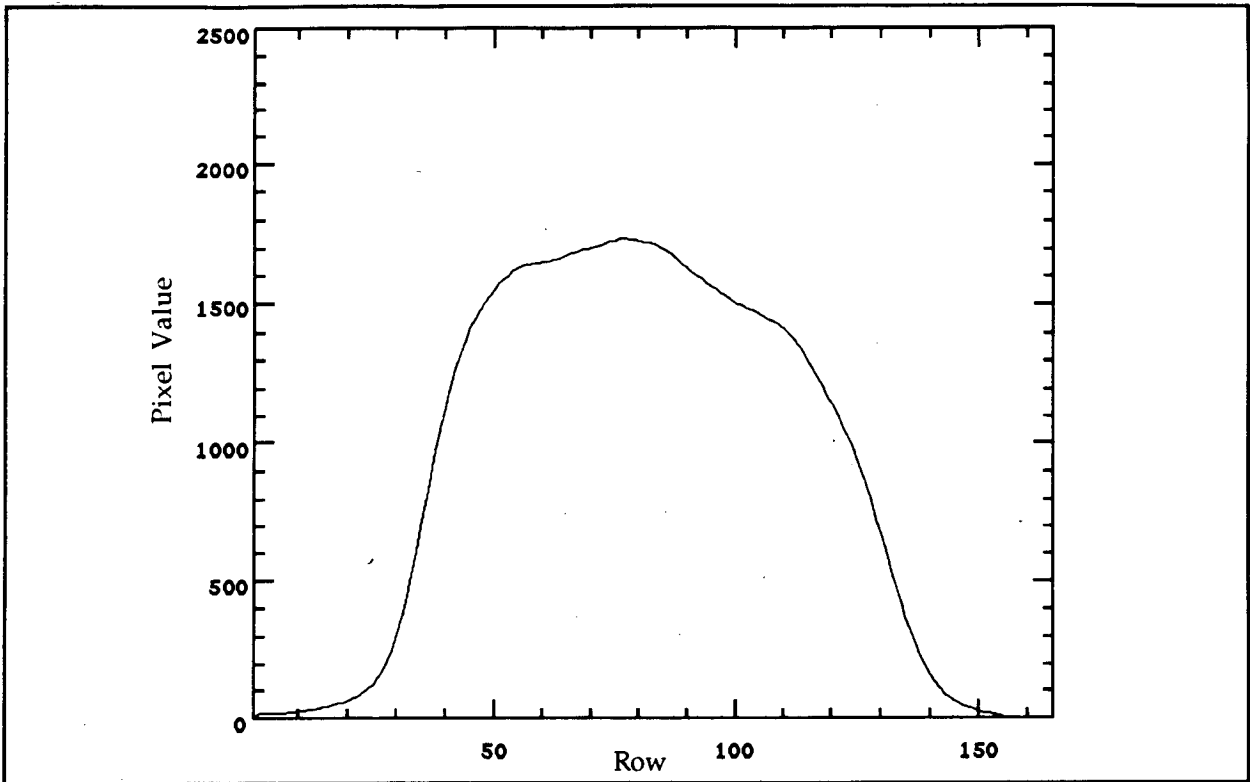


Figure 5. Average Column Minus Background for 2/18/92.

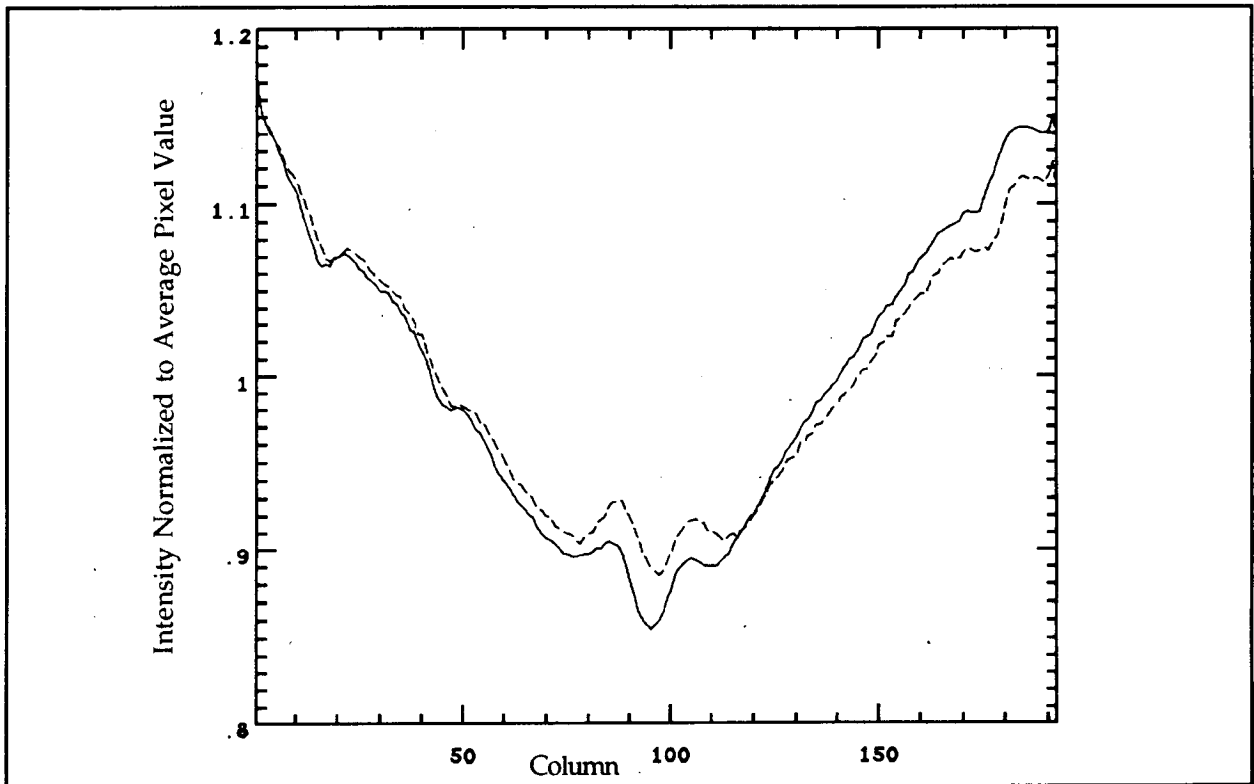


Figure 6. Comparison of Zeroed and Normalized Ca K Profiles of 2/18 (First Image) and 2/28.

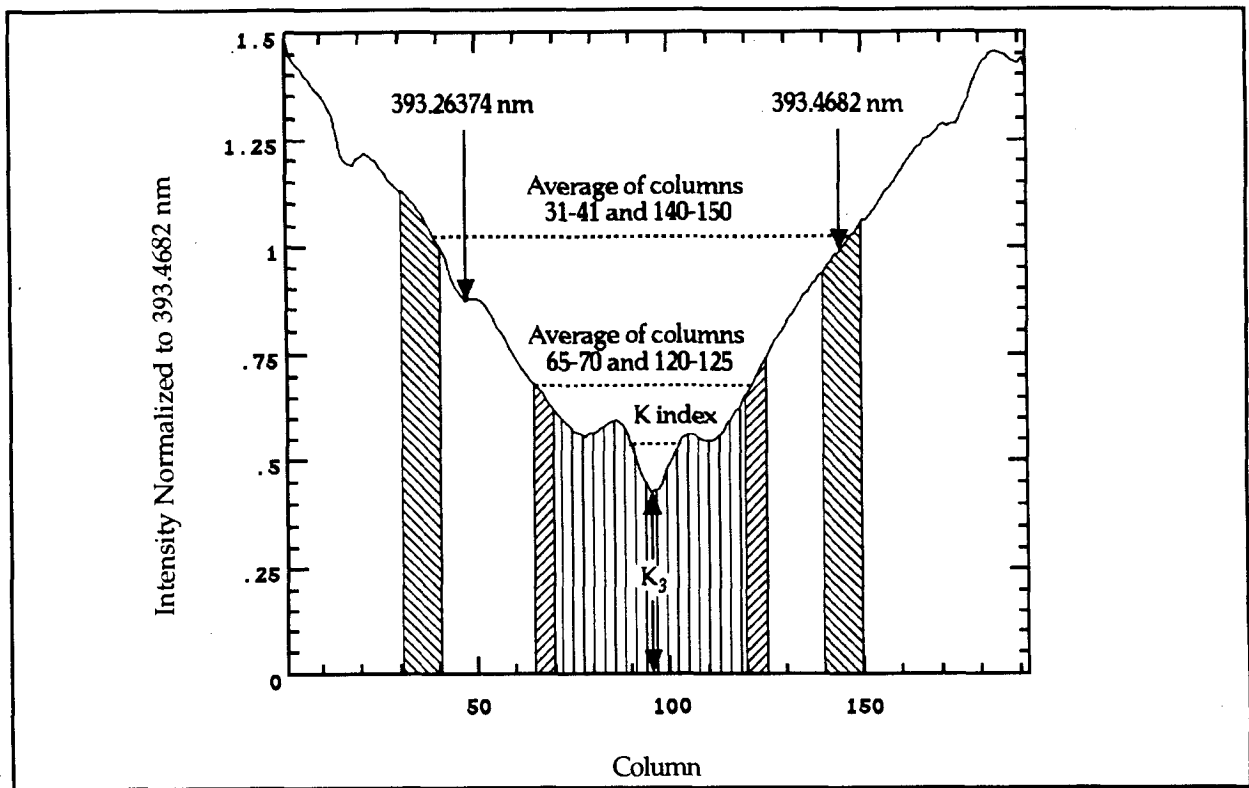


Figure 7. Ca K Profile from 2/18 Showing Averaged Columns and Important Wavelengths and Values.

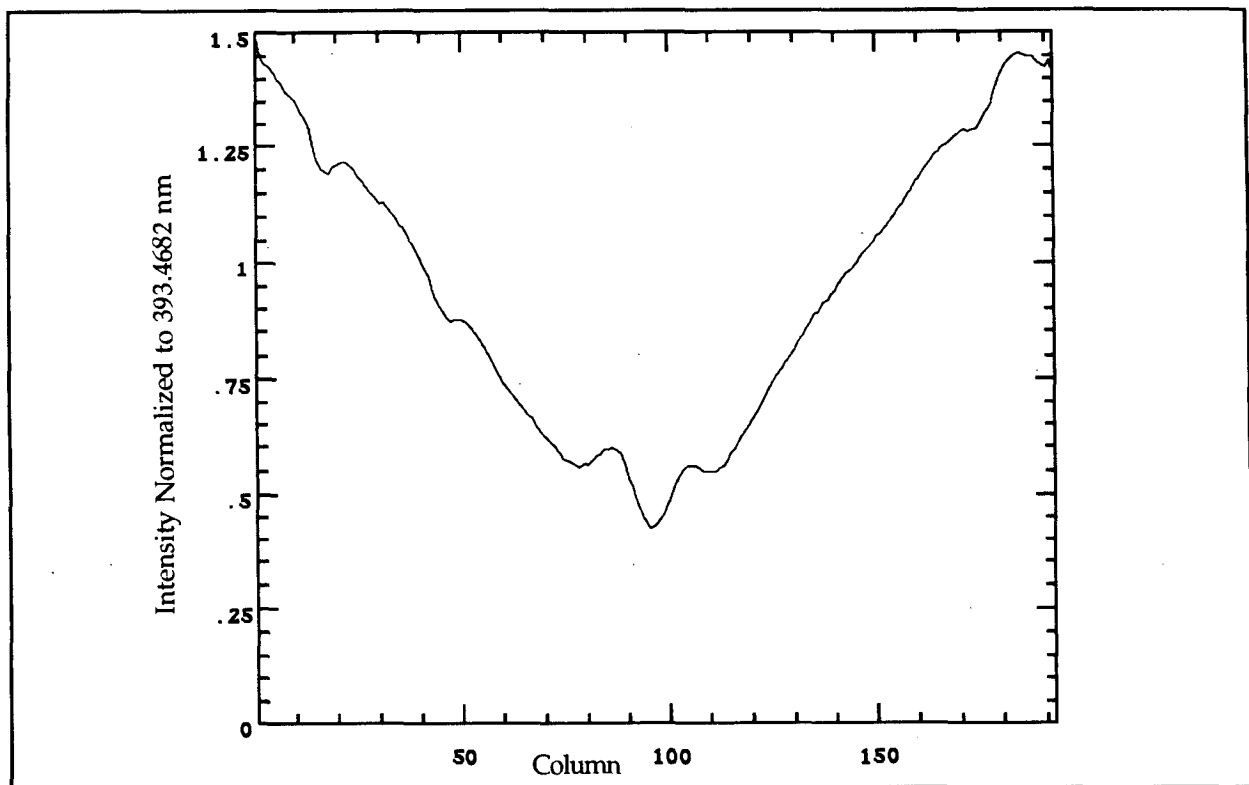


Figure 8a. Ca K Profile for 2/18.

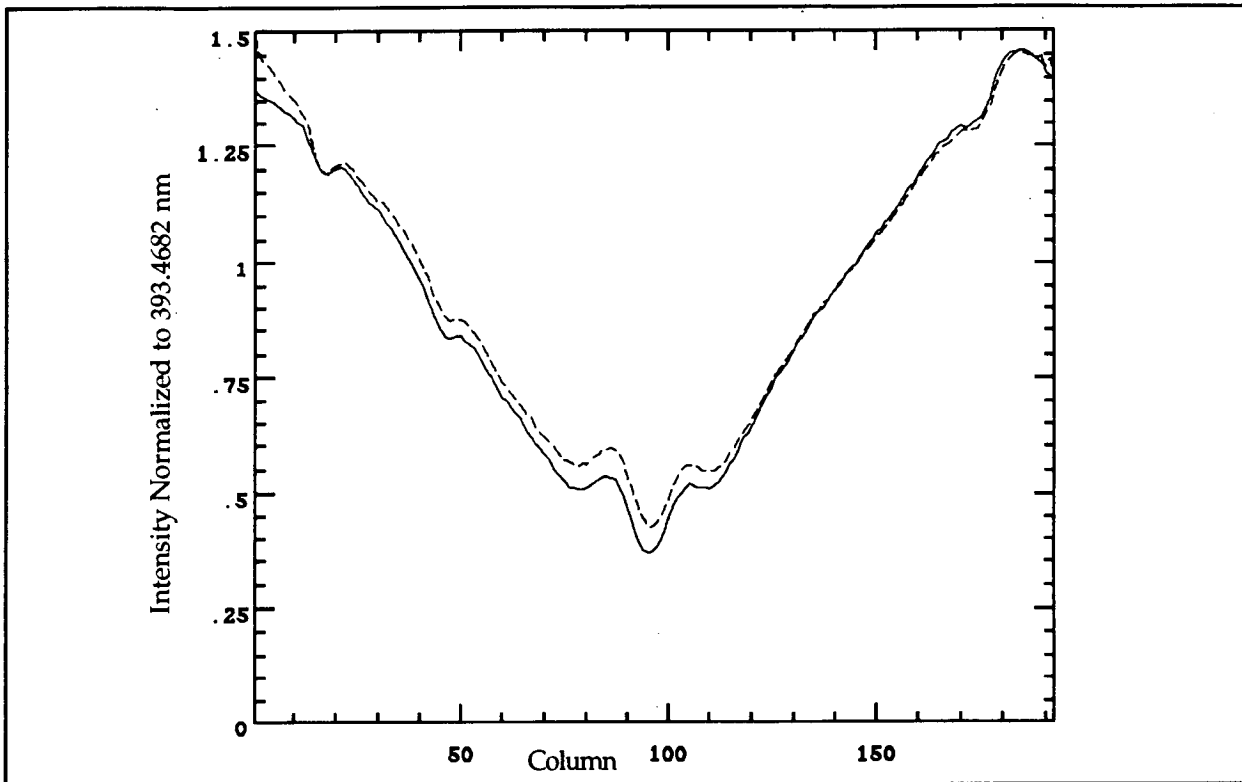


Figure 8b. Ca K Profile for 2/20 (with 2/18 comparison).

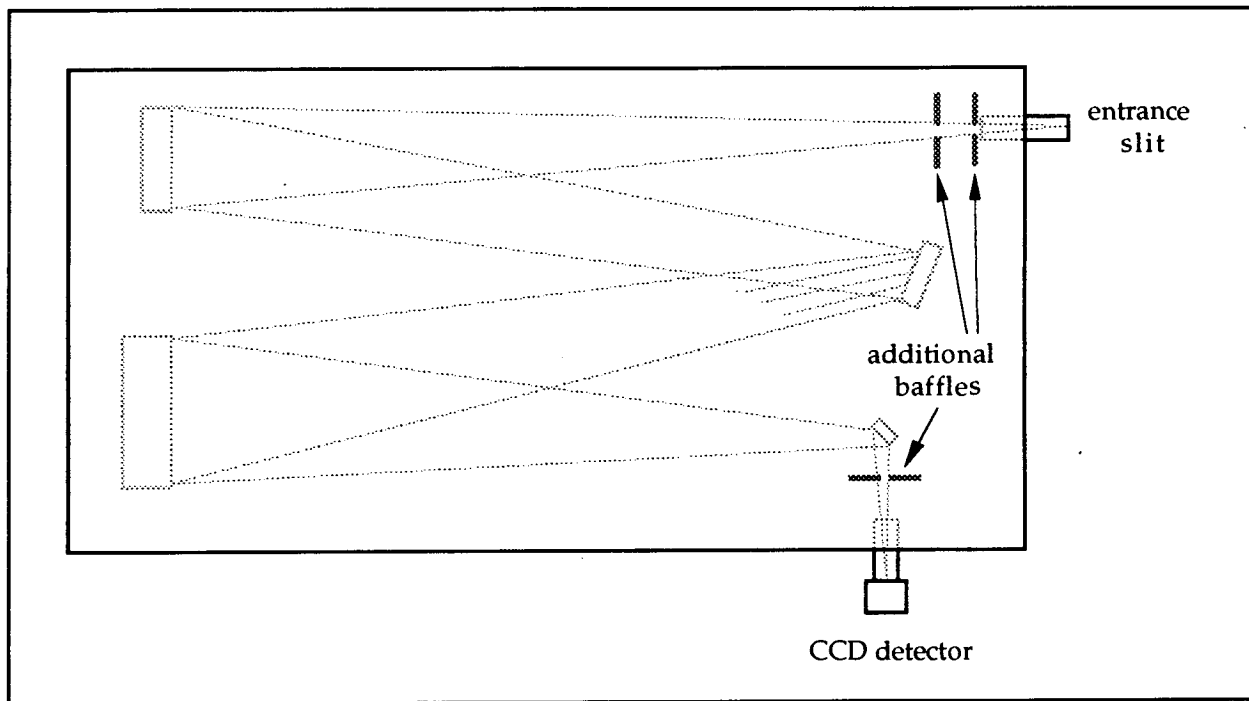


Figure 9. Positions for additional baffles to reduce scattered light.